Final copy

533418

Corrosion Issues for Ceramics in Gas Turbines

Nathan S. Jacobson, Dennis S. Fox, and James L. Smialek
NASA Glenn Research Center
Cleveland, OH 44135 USA

Elizabeth J. Opila
Cleveland State University/NASA Glenn Research Center
Cleveland, OH 44135 USA

Peter F. Tortorelli and Karren L. More
Oak Ridge National Laboratory
Oak Ridge, TN 37831 USA

Klaus G. Nickel
Eberhard-Karls-Universitat Tubingen
D-72074 Tubingen, Germany

Takehiko Hirata
Mitsubishi Heavy Industries, Ltd.
Yokohama, Japan

Makoto Yoshida
Kyocera Corporation
Kagoshima, Japan

Isao Yuri
Central Research Institute of Electric Power Industry
Kanagawa, Japan

INTRODUCTION

Historical and Programmatic Perspective

The requirements for hot-gas-path materials in gas turbine engines are demanding. These materials must maintain high strength and creep resistance in a particularly aggressive environment. A typical gas turbine environment involves high temperatures, rapid gas flow rates,

high pressures, and a complex mixture of aggressive gases. Figure 26.1 illustrates the requirements for components of an aircraft engine and critical issues [1]. Currently, heat engines are constructed of metal alloys, which meet these requirements within strict temperature limits. In order to extend these temperature limits, ceramic materials have been considered as potential engine materials, due to their high melting points and stability at high temperatures. These materials include oxides, carbides, borides, and nitrides. Interest in using these materials in engines appears to have begun in the 1940s with BeO-based porcelains [2]. During the 1950s, the efforts shifted to cermets. These were carbide-based materials intended to exploit the best properties of metals and ceramics. During the 1960s and 1970s, the silicon-based ceramics silicon carbide (SiC) and silicon nitride (Si_3N_4) were extensively developed.

Although the desirable high-temperature properties of SiC and Si_3N_4 had long been known, consolidation of powders into component-sized bodies required the development of a series of specialized processing routes [3]. For SiC, the major consolidation routes are reaction bonding, hot-pressing, and sintering. The use of boron and carbon as additives which enable sintering was a particularly noteworthy advance [4]. For Si_3N_4 the major consolidation routes are reaction bonding and hot pressing [5]. Reaction-bonding involves nitridation of silicon powder. Hot pressing involves addition of various refractory oxides, such as magnesia (MgO), alumina (Al_2O_3), and yttria (Y_2O_3). Variations on these processes include a number of routes including Hot Isostatic Pressing (HIP), gas-pressure sintering, sinter-HIPing, and Encapsulation-HIPing. It is important to note that each process involves the addition of secondary elements, which later were shown to dramatically influence oxidation and corrosion behavior.

As dense bodies of silicon-based ceramics became more readily available, their desirable high temperature properties were confirmed. These materials retained strength to very high temperatures (i.e. 1300-1400°C). Further, they were lightweight and made from abundant materials. SiC and Si_3N_4 therefore emerged as leading ceramic candidates for components in heat engines, designed to operate at higher temperatures for better performance and fuel efficiency. The first US programs for ceramics in heat engines have been reviewed [6]. Selected programs on ceramic engine parts are summarized here in regard to their contributions to understanding the corrosion behavior of ceramics in a heat engine environment.

The first major United States program was funded by DARPA (Defense Advanced Research Projects Agency) and involved the U.S. Army, Westinghouse Research Laboratories (Pittsburgh, PA), and Ford Motor Company (Dearborn, MI) in the early 1970s. The Westinghouse element involved power generation turbine vanes and the Ford element involved automotive engines. Several significant studies on the oxidation of additive-containing SiC and Si_3N_4 were done at

Westinghouse [7, 8]. These studies showed the additives controlled oxidation, as will be discussed in more detail later in this chapter.

During the 1970s, DARPA and NAVSEA (Naval Sea Systems Command) also funded a Ceramic Gas Turbine Engine demonstration program [9], which was conducted primarily at Garrett Turbine Engines (Phoenix, AZ). An AiResearch Turboprop Engine was selected for combustor and turbine redesign with ceramics. Numerous processing and property measurement studies were a part of this program. Oxidation and salt-induced corrosion tests were done on hot pressed and reaction-bonded Si_3N_4. For hot-pressed Si_3N_4 in pure oxygen at temperatures below ~1100°C, strength actually increased due to surface flaw healing. However, higher temperature oxidation and salt-induced corrosion led to surface pitting and strength degradation [10].

Also in the 1970s, as part of the Department of Energy (DOE) Ceramic Technology Readiness (CTR) program, a corrosion/erosion study of various commercially available ceramic materials was conducted [11]. Various types of SiC and Si_3N_4, as well as AlN, Al_2O_3-ZrO_2, Al_2O_3-SiC, $MgAl_2O_4$ and SiAlON were examined after exposure to laboratory air environments and also coal-derived combustion environments. Damage was assessed from strength degradation and microscopic examination. Combustion environments led to more severe corrosion than laboratory air environments. This was attributed to water vapor and thermal cycling in the combustion environments. Unprotected AlN experienced particularly severe degradation and was determined to be unsatisfactory for combustion applications.

There was also an interest in the development of oxide ceramics for heat-exchangers in automotive turbines. Lithium aluminum silicate (LAS) was selected due its low thermal expansion. A substantial testing program at Ford dating back to 1965 on LAS regenerators identified thermal stress and chemical attack as the two major modes of failure [12]. On the cold side of the regenerator, sulfuric acid forms and attacks the ceramic; on the hot side, sodium from fuel impurities attacks the ceramic. Other low thermal expansion oxides, such as magnesium aluminosilicate (MAS) and aluminosilicate (AS), were subsequently developed to minimize these problems.

Several programs were initiated that specifically focused on ceramics for automotive applications. The first was the Ceramic Automotive Turbine Engine (CATE) program in the late 1970s and early 1980s, which was funded by the National Aeronautics and Space Administration (NASA) and DOE and performed primarily at Detroit Diesel Allison. The emphasis here was on sintered SiC and Si_3N_4. Later, DOE and NASA funded the Automotive Gas Turbine (AGT) program [13]. This program involved development of both a MAS ceramic recuperator and SiC turbine blades.

The AGT program later became the Advanced Turbine Technology Applications Program (ATTAP), which was aimed more at component development [14].

Related to these programs were 3500 hr durability tests at Garrett, funded by NASA. These involved cyclic oxidation tests on a variety of commercial SiC and Si_3N_4 materials [15, 16]. Tests were conducted in a diesel fuel burner with exposures at 1204 and 1371°C and cooling to below 204°C. Five cycles per hour were run with durations to 3500 hr. The materials tested showed good strength retention. As part of the AGT and ATTAP programs, salt corrosion tests were run at NASA Lewis Research Center (Cleveland, OH). Particular care was taken to understand the deposition parameters. It was found that basic molten salt deposits led to severe surface pitting and strength degradation [17, 18].

Concurrent to the engine development programs were programs at DOE/Oak Ridge National Laboratory (ORNL) in the 1980s and 1990s for ceramic heat exchangers in various types of elevated temperature industrial applications. These combustion environments are low-velocity as compared to heat engines. These studies again showed that pure oxidation was not a significant issue for ceramics, but deposit-induced corrosion and water vapor were quite important. Further a basic oxide deposit was particularly detrimental [19].

A significant international program from 1979-1993 was "Program of Research and Development on High Temperature Materials for Automotive Engines" of the International Energy Agency (IEA), which involved Germany, U.S., Sweden and Japan. The programs of the European Communities had ceramics for turbines as one focus within the larger program "Basic Research in Industrial Technologies for Europe / European Research on Advanced Materials" (Brite/EuRam) in the 1990s. The most significant national German program was funded from 1985-1994 [20]. It led to basic insight into the complex scale structures on additive containing Si_3N_4 and early attempts to model corrosion kinetics [21].

In Japan there have been a number of studies for development of ceramics in gas turbines, including corrosion studies. A 300 kW class Ceramic Gas Turbine (CGT) program (1998-1999), which is administered by the New Energy and Industrial Technology Development Organization (NEDO) under the sponsorship of the Ministry of International Trade and Industry (MITI), developed the ceramic gas turbines for cogeneration [22] and demonstrated excellent high temperature strength of a fine-grained Si_3N_4 with a stable rare earth disilicate grain boundary phase [23, 24]. In addition the Petroleum Energy Center (PEC) and the Japan Automobile Research Institute (JARI) developed a 100 kW ceramic gas turbine for automobiles [25], under a MITI-sponsored program (1990-1997). There was also a program for large-scale gas turbines

under the Central Research Institute of the Electric Power Institute (CRIEPI) and Hitachi, Ltd. [26, 27]. Another program was under the Tokyo Electric Power Co. (TEPCO) [28]. Related to these programs were corrosion studies showing the deleterious effects of molten salts on the strength of SiC and Si_3N_4 [29].

In the late 1980s and 1990s several significant changes occurred which influenced the direction of ceramic corrosion studies.

1. The availability of pure, free-standing SiC and Si_3N_4 led to fundamental studies of oxidation of these materials. It was now possible to get accurate kinetic rates and product compositions without the influence of additives.
2. The importance of complex combustion environments was recognized. While simple isothermal oxidation tests provide useful fundamental information, actual engine environments are quite complex--consisting of water vapor, possible condensed phase deposits as well as high pressures and thermal cycling [1]. Resistance to pure oxygen at constant temperatures is not sufficient; other factors must be considered.
3. Ceramic matrix composites (CMCs) were developed. Continuous fiber reinforced ceramics offer a good deal of promise for improved fracture toughness. They are based on a carbon or SiC fiber in a SiC or Si_3N_4 matrix. For the SiC fiber composites, the fiber is coated with a carbon or boron nitride layer to allow proper load transfer to the fiber. The problem area is the carbon or boron nitride, which readily oxidize. Recent oxidation studies focus on these issues.

Major ceramic engine programs in the 1990s focused on CMCs were the NASA Enabling Propulsion Materials (EPM) program [30] and the DOE Continuous Fiber Ceramic Composite (CFCC) program [31]. The NASA EPM program centered on the use of a SiC-fiber/SiC-matrix for a high temperature, backside cooled combustor liner, for aircraft engine applications. In burner studies, which simulated the EPM environment, high pressure water vapor was shown to be a significant corrodent [32, 33], resulting in increased recession of monolithic SiC. This was consistent with several Japanese studies which showed increased recession rates of SiC and Si_3N_4 in combustion environments [34, 35]. This recession is related to water-enhanced volatilization and will be discussed in more detail in the next section.

The DOE CFCC program was more generic and directed at CMCs for a variety of industrial applications. In the later 1990s DOE together with Solar Gas Turbines, Inc. began a demonstration program for a ceramic stationary gas turbine (CSGT) for both power and steam generation [36-38]. In this program, ceramic parts are substituted for metallic hot-section parts such as blades, nozzles, and combustor liners. Long-term tests of two types of ceramic components have been conducted without component failure; nevertheless, significant

degradation was observed. Solar Turbines, Inc. (San Diego, CA) tested several SiC/SiC composite combustor liners for times up to 5028h in a Centaur 50S ground-based power unit (Texaco – Bakersfield, CA) [36,37]. Microstructural evaluation showed excessive material recession in hot, high velocity sections of the liners. Rolls-Royce Allison (Indianapolis, IN) has tested an AS800 Si_3N_4 first stage vane assembly in a Model 501-K turbine (Exxon – Mobile, AL) for 815 h [38]. Dimensional measurements found significant material recession at the mid-span of the trailing edge of the vanes with even greater losses at the vane leading edges. The recession in both field tests was attributed to volatility of the silica scale in the high water vapor partial pressure, high gas velocity environments as discussed later.

The development of CMCs in France for the Hermes program and in the U.S. for the EPM and CFCC programs led to several studies of the unique issues in CMC oxidation. At their current state of development CMCs are based on either a carbon fiber in a SiC matrix or a SiC fiber in a SiC or Si_3N_4 matrix. The SiC fiber must be coated with carbon or boron nitride. Thus all types of CMCs contain a second phase, which oxidizes easily. Initial studies were on composites of SiC matrices with carbon fibers [39, 40] and carbon-coated SiC fibers [41, 42]. Later studies were on SiC matrices with BN-coated SiC fibers [43-45]. The final stage of CMC processing involves the application of a seal coating—typically CVD SiC—over the matrix. If this seal coat remains intact, the carbon or BN is not exposed to oxidation. However, in the event of seal coat damage in service, oxidation of the carbon or BN becomes a major problem.

In summary, oxidation/corrosion studies have been included in many ceramic engine development programs. While many of these are system specific, it is possible to draw some general conclusions:

1. SiC, Si_3N_4, and composites of these appear to be the most promising ceramics for hot stage applications. AlN undergoes substantial degradation in combustion environments and is not a suitable candidate.
2. SiC and Si_3N_4 show slow oxidation kinetics and good strength retention in purely oxidizing environments.
3. On some materials low temperature oxidation heals surface flaws and actually improves strength. However higher temperature oxidation creates surface pits and leads to strength degradation.
4. Basic molten salt or oxide deposits lead to surface pitting and strength degradation.
5. The water vapor present in a combustion environment enhances degradation.
6. The effects of temperature cycling also appear to be material dependent. In some cases cycling has little effect; in other cases it may lead to degradation.

7. The major issue with CMCs is oxidation of the fiber coating. This is due to an inadequate external coat—either not initially formed properly or damaged in service.

In the next section, we focus on these key issues and the chemistry behind these issues.

Experimental Methods

Accurate simulation of engine environments in a laboratory environment is a major issue. Actual engine tests are expensive and it is difficult to accurately control all variables. It is important to simulate the high temperatures, pressures, flow rates, and gas compositions found in an engine. The most common method is the burner rig, shown schematically in Figure 26.2 [1]. Over the years burner rigs have evolved into more controlled test systems [46]. Although these rigs are well accepted for materials testing now, their very nature prevents them from offering the precise control of a laboratory furnace.

Laboratory tests in electric furnaces are substantially less expensive than burner rig tests. Yet they cannot fully simulate the engine environment. The investigator is often able to determine the critical issues from the burner and focus on this with a laboratory furnace [1].

Another important issue is the assessment of corrosion damage. Weight change is most commonly used, but this does not give an indication on the form of surface or internal damage. Examination of oxide and matrix morphologies with techniques such as optical microscopy as well as scanning and transmission electron microscopy is necessary. Measured reduction of load-bearing capability is another useful indication of corrosion damage.

CORROSION MECHANISMS FOR SILICON-BASED CERAMICS

Baseline Oxidation Data

Isothermal oxidation data for high purity SiC and Si_3N_4 in pure, dry oxygen provide a useful baseline of the slowest possible material consumption rates, as illustrated in Figure 26.3 [47]. The key oxidation reactions are:

$$\text{Oxidation of SiC:} \quad SiC(s) + 3/2\ O_2(g) = SiO_2(s) + CO(g) \tag{1}$$

$$\text{Oxidation of } Si_3N_4\text{:} \quad Si_3N_4(s) + \tfrac{3}{4}\ O_2(g) = 3/2\ Si_2N_2O(s) + \tfrac{1}{2}\ N_2(g) \tag{2}$$

$$Si_2N_2O(s) + 3/2\ O_2(g) = 2\ SiO_2(s) + N_2(g) \tag{3}$$

There is general agreement that for SiC and Si_3N_4, oxygen diffusion inward through the growing scale is rate controlling [1, 48]. This leads to the familiar parabolic kinetics [47] where the rate slows as the oxide scale thickens:

$$x^2 = k_p t \tag{4}$$

Here x is scale thickness, k_p is the parabolic rate constant, and t is time.

As shown in 26.3 [47], the rates of oxidation for pure Si_3N_4 are slower than for pure SiC in pure oxygen. The formation of an inner layer of silicon oxynitride appears be a factor in the slower oxidation rates [50], although the exact mechanism for this is still controversial [1, 48, 51].

In practical situations, the differences between SiC and Si_3N_4 would not be observed [52]. Instead the additives to these ceramics and effects of other combustion gas components (e.g. water vapor, metallic impurities) tend to dominate oxidation behavior.

Material Effects on Oxidation

Additive-Containing SiC and Si_3N_4

Many of the early oxidation studies of SiC and Si_3N_4 were on additive-containing materials. For SiC materials, the most common additives are boron, carbon, and/or alumina. A common form of sintered α-SiC contains B_4C. This SiC material oxidizes at rates similar to CVD SiC [47, 53]. Hot pressed SiC generally requires alumina additives. The oxidation of alumina-containing SiC has been extensively studied. The alumina tends to migrate to the oxide scale. This leads to local crystallization and even mullite formation if the alumina concentration is sufficiently high. Oxidation rates tend to increase with increasing alumina content, as shown in Figure 26.4 [7].

Nearly all commercial forms of Si_3N_4 require refractory oxide additions to promote densification. Cubiciotti and Lau have demonstrated that these additives dominate oxidation behavior to the point where the metal cation diffusion outward is rate controlling [54, 55]. These oxidation rates are substantially higher than those observed with pure Si_3N_4. Figure 26.5 illustrates the oxide film on a Si_3N_4 with Y_2O_3 additives—note the two phases. In multiphase materials, a variety of processes act simultaneously (e.g. internal and external oxidation, grain boundary widening, migration of additives to the scale, porosity formation, and scale crystallization). It may not be possible to model these with a simple rate law [21]. More complex expressions may be

necessary [56]. Both the total amount and specific composition of the additives are critical. Some compositions of Si_3N_4 with Y_2O_3 sintering aids result in grain boundary phases which undergo a volume expansion on oxidation. This leads to disintegration of the sample [57].

Some processing routes lead to porous ceramics, such as reaction-bonded Si_3N_4. Although less favorable for candidate heat engine components, these materials may be less expensive than their dense counterparts. Oxidation studies indicate that internal oxidation is a critical issue and controlled by pore diffusion [58, 59].

Continuous Fiber-Reinforced Composites

As discussed in the introduction, continuous fiber-reinforced composites represent a large area of research in silicon-based ceramics. One area of major interest is in carbon fiber-reinforced SiC composites. This is due to the stability of carbon fibers to high temperatures in inert environments. The problem is that the carbon fibers oxidize quite readily in the event of a crack in the SiC matrix and subsequent exposure of these fibers to oxidizing gases. Lamouroux, et al. [39, 40] conducted both an experimental and theoretical study of the oxidation of two dimensional carbon fiber-reinforced SiC composites. Basically they observe three oxidation regimes: I) Low temperature ($T < 800°C$): overall kinetics are limited by the reaction of carbon and oxygen II) Intermediate temperatures ($800°C < T < 1100°C$): overall kinetics are limited by diffusion of CO and CO_2 from carbon oxidation out of pores and microcracks in the SiC matrix and III) High temperatures ($T > 1100°C$): kinetics are dominated by sealing of the SiC matrix due to SiO_2 formation. More recently Halbig and Cawley [60] have modeled the oxidation of carbon fibers exposed to oxygen due to a matrix crack. They also see the important effect of reaction control at low temperatures and diffusion control at high temperatures. Although carbon fiber-reinforced SiC has attractive mechanical properties, the susceptibility of the carbon fiber to oxidation is a major limitation. Lamouroux, et al. [61] have proposed a multilayer matrix with improved oxidation resistance. More research is needed on improved oxidation resistance of carbon fiber-reinforced SiC to make this material viable.

A second area of interest is SiC-fiber/SiC or Si_3N_4 matrix reinforced composites. SiC fibers stable to high temperatures ($T > 1200°C$) have been developed. Although they are still quite expensive, they eventually are expected to decrease in price. A SiC fiber-reinforced SiC composite is shown schematically in Figure 26.6 [62]. A major problem with these types of composites is the rapid oxidation of the C or BN fiber coating. Several elegant models have been developed for this oxidation process [39, 40, 63], but there are currently no complete solutions to the problem of rapid oxidation of the fiber coating.

Consider first the SiC system with carbon-coated fibers. Figure 26.7 shows some typical oxidation curves for carbon coated SiC fiber in a reaction-bonded Si_3N_4 matrix [64]. At low temperatures the carbon coatings oxidize readily leading to the observed weight losses. At high temperatures a protective oxide film grows on the outside of the composite, leading to protection of the interior. However, protection would be negated if a large matrix crack forms when the ceramic is under load. This situation has been modeled by Filipuzzi and co-workers [41, 42] and is shown schematically in Figure 26.8. The oxygen pressure dependence of SiC oxidation indicates that most of the oxidation occurs near the mouth of the pore. The process modeled includes these steps:

--Diffusion of oxygen into the pore.
--Two step oxidation of carbon to CO and CO_2.
--Diffusion of CO out of the pore.
--Consumption of oxygen by oxidation of the matrix.
--Consumption of oxygen by oxidation of the fiber.

Other investigators have extended this model to regimes where reaction control of carbon oxidation is important [63]. These models have been helpful in explaining the oxidation results and high-temperature environmental effects on mechanical properties.

The other commonly used fiber coating is hexagonal boron nitride. Oxidation of this material is complex and several degradation routes are possible [45] as shown in Figure 26.9. As the BN and the SiC oxidize, both B_2O_3 and SiO_2 are formed. These react to form low melting borosilicates, as illustrated in Figure 26.9(a). Compare this to the second type of degradation behavior. Boria (B_2O_3), the oxidation product of BN, reacts readily with water vapor found in the combustion environment to form highly stable $H_xB_yO_z(g)$ species. Thus the BN fiber coatings volatilize in a way analogous to carbon, but due to the reaction with water vapor. This explains the appearance of Figure 26.9(b). Moving down the annular region of Figure 26.9(b), into the composite, one would eventually reach the remaining BN coating. These fiber coating recession distances can be determined and related to simple diffusive fluxes through contracting annular pores [45]. This is illustrated in Figure 26.10.

Effect of Oxidation on Mechanical Properties

The effect of oxidation on strength is critical to determine the ceramic's suitability for an engine component. Consider first monolithic ceramics. As discussed in the Introduction, under some

conditions mild oxidation can heal surface flaws and lead to a strength increase; whereas more severe oxidation can lead to pitting and strength decreases [10]. This has been verified and further explored with laboratory studies [65, 66]. These issues have been discussed in detail in a review by Tressler [67].

In an actual engine environment, a component would be simultaneously exposed to both oxidation and mechanical stress. There are several studies of stress-enhanced oxidation of monolithic Si_3N_4 in the literature [68, 69]. There is a complex interaction between stress and oxidation. Stresses form microcracks and cavities and also alter diffusivities. Each of these factors tends to enhance oxidation. Wereszczak, et al. [69] have observed the formation and growth of stress-corrosion cracks which ultimately led to failure. Thümmler and Gratwohl [70] have shown that oxidation of certain additive-containing Si_3N_4 compositions leads to formation of a softened grain boundary phase and consequently enhanced creep. SiC compositions without additives show better overall creep resistance and less susceptibility to oxidation effects on creep.

There is a good deal of literature on the mechanical properties of fiber-reinforced CMCs in oxidizing environments. Halbig, et al. [71] have examined oxidation of carbon fiber-reinforced CMCs under stress. Time-to-failure is dramatically reduced due to oxidation of the carbon fiber through an opened crack. The major problem occurs in the intermediate temperature (~500-1000°C) regime when the amount of SiO_2 formed is insufficient to seal cracks in the SiC matrix. Stress-rupture studies of SiC-fiber/carbon/SiC matrix [72] and SiC-fiber/BN/SiC matrix [73] CMCs all indicate that oxidation of the fiber coatings (carbon or boron nitride) is the major cause of failure. Development of oxidation-resistant fiber coatings is a critical area of research and presents major challenges.

Complex Corrosion Environments

The discussion thus far has focused primarily on isothermal oxidation in pure oxygen. However, there are many other factors in the environment of a heat engine. These include thermal cycling, additional oxidants such as H_2O and CO_2, aggressive low-level gases such as SO_2 and HCl, and corrosive deposits such as sulfates and vanadates. To some degree, these are dependent on the type of heat engine. Aircraft gas turbines involve daily thermal cycling, whereas cycling would be limited in utility turbines. A coastal-based turbine is more susceptible to salt attack than a turbine located inland. Nonetheless, some general comments can be made about combustion environments. Table 26.I lists some properties of common hydrocarbon fuels [74-78]. Note that all contain impurities, which may be corrosive at high temperatures. Figure 26.11 is a plot of

equilibrium gas composition and adiabatic flame temperature as function of equivalence ratio [1]. The fuel used for this calculation is a typical aviation fuel - Jet A, but the results are similar for any type of hydrocarbon fuel. Note that H_2O and CO_2 are always present in amounts of about 10%. In a fuel lean environment (Equivalence Ratio < 1), which is most common, O_2 is also present. In a fuel-rich environment (Equivalence Ratio > 1), the O_2 content is very low and CO and H_2 become important.

In the following section, each of the additional factors, beyond isothermal oxidation, will be discussed for SiC and Si_3N_4.

Cyclic Oxidation

When samples oxidize during thermal cycling, stresses develop due to the coefficient of thermal expansion (CTE) mismatch between the silica scale and the SiC or Si_3N_4 substrate. These mismatches are illustrated in Figure 26.12 [48]. In actual engine environments, partially or fully crystalline scales are expected to form. Compressive stresses are expected on heating and then tensile cracks on cooling. On heating the compressive stresses can lead to crack healing. Hence SiC and Si_3N_4 show good behavior in cyclic oxidation, unlike their superalloy counterparts which often show scale buckling and spallation due to compressive scale stresses on cooling. Figure 26.13 illustrates the good oxidation behavior of some types of SiC and Si_3N_4 during thermal cycling [48].

Water Vapor

As discussed in the Introduction, the burner rig studies clearly suggest that water vapor in the combustion environment degrades silicon-based ceramics. Laboratory experiments have shown that water vapor has three major effects on the oxidation of silicon-based ceramics. First, water vapor enhances the transport of impurities to the ceramic surface. This may occur by formation of gaseous hydroxides, such as NaOH, from metallic impurities in the environment. Impurities become incorporated in the silica scale, thereby increasing the oxidation rate substantially compared to the low rates observed under very clean conditions [79]. This is discussed further in the section on low-level metal cation impurities.

Second, water vapor increases the intrinsic oxidation rate of silica-formers compared to rates observed in dry oxygen. This mechanism has been described by Deal and Grove [80]. While the diffusivity of the water molecule in silica is about one order of magnitude lower than that of

molecular oxygen, the solubility of water in silica is almost three orders of magnitude higher than that of oxygen. Since the parabolic rate constant is equal to the product of the diffusivity and the solubility, the parabolic rate constant for silica formation is higher in water vapor than in dry oxygen. Oxidation of silicon carbide in water vapor occurs by the reaction:

$$SiC(s) + 3H_2O(g) = SiO_2(s) + CO(g) + 3H_2(g) \quad (5)$$

One consequence of these higher oxidation rates is the generation of more product gases. The silica scale under these conditions often contains bubbles and pores formed by release of these gases [81]. Since the parabolic oxidation rate increases with water vapor partial pressure, high-pressure exposures of silicon carbide and silicon nitride in water vapor result in the formation of silica scales riddled with bubbles and pores. These bubbles and pores make the silica scale non-protective and very high oxidation rates are then observed [81, 82].

Finally, water vapor causes volatilization of the silica scale by the reaction [83, 84]:

$$SiO_2(s) + 2H_2O(g) = Si(OH)_4(g) \quad (6)$$

Since this volatilization occurs simultaneously with the oxidation reaction (Equation 5), the resulting kinetics follow a paralinear rate law given by:

$$\frac{dx}{dt} = \frac{k_p}{2x} - k_l \quad (7)$$

where x is the scale thickness, t is time, k_p is the parabolic oxidation rate constant, and k_l is the linear volatilization rate constant. Paralinear kinetics can be monitored by either substrate recession measurements or weight change as shown in Figure 26.14 [48]. Typical paralinear weight change behavior is shown (Figure 26.15) for silicon-based materials exposed in a laboratory furnace containing water vapor [48]. At long times or high volatility rates, paralinear kinetics result in linear recession of the ceramic material, and a constant oxide thickness, as well as linear weight loss [32, 34, 35]. Under these conditions, the recession and weight loss are limited by the transport of $Si(OH)_4(g)$ away from the ceramic through a gaseous boundary layer. This has been modeled using the following expression [33]:

$$k_l = 0.664\ Re^{1/2}\ Sc^{1/3}\ \frac{D\rho}{L} \quad (8)$$

where Re is the Reynold's number, Sc is the Schmidt number D, is the interdiffusion coefficient of $Si(OH)_4$ in the boundary layer gas, ρ is the concentration of $Si(OH)_4$ at the silica/gas interface and L is a characteristic length. This expression can be reduced to terms that describe the combustion environment such as pressure, P, gas velocity, v, and material temperature, T, so that

$$k_l \propto \exp\left(\frac{-\Delta H_f}{RT}\right) P^{1.5} v^{0.5} \tag{9}$$

Here R is the gas constant. The temperature dependence arises from the enthalpy of formation (ΔH_f) of $Si(OH)_4$ according to the reaction given in Equation 6 [33]. The pressure dependence of SiC weight loss and recession has been demonstrated experimentally in a High Pressure Burner Rig at the NASA Glenn Research Center [32], as shown in Figure 26.16. The data, normalized by the $P^{1.5}v^{0.5}$ term fit the model based on equation (8) quite well for a variety of pressures and velocities, as shown in Figure 26.17 [32]. The high pressures, high temperatures, and high velocities present in gas turbine applications thus all promote water vapor attack of silicon-based ceramics.

Recession consistent with the volatilization mechanism has been observed in two recent engine field-tests as previously mentioned. Figure 26.18 shows recession and porous glass formation for a SiC/SiC combustor liner exposed for 2300 hrs in a land-based turbine (T_{max}=1150°C, P=10 atm, v=61m/s). Figure 26.19 shows the measured recession at the mid-span trailing edge of AS800 Si_3N_4 vanes exposed for 815 h in a land based turbine (T_{max}=1260°C, P=8.9atm, v_{max}= 573m/s). The scatter is attributed to vane-to-vane temperature variation. The measured recession rates are consistent with rates calculated for a range of temperatures using a model of the type given by Equation 9. Figure 26.20 shows the dimensional change for a single vane at mid-span before and after engine testing for 815 h. Figure 26.21 shows that the recession at the leading edge exceeds the rate found elsewhere on the vane. Other mechanisms such as erosion or viscous flow may also be important here.

Because of the extensive degradation that occurs in turbine environments, as demonstrated in these field-tests, environmental barrier coatings (EBCs) are needed for SiC and Si_3N_4 turbine components. An EBC coated SiC/SiC combustor liner is currently undergoing field-testing and has successfully completed 12,000h without observable recession problems (private communication, M.K. Ferber). EBCs therefore show promise for limiting recession due to silica volatility. Discussion of these coatings is included in another chapter in this volume.

Oxidation by CO_2

As previously shown in Fig. 26.11 [1], CO_2 is present in all combustion environments. The presence of this gas in the combustion environment has not been shown to affect the durability of silicon-based ceramics. Figure 26.22 shows that the effect of CO_2 as an oxidant is negligible compared to water vapor and even oxygen [85].

Attack from Aggressive Gases such as HCl and SO_2

Although HCl and SO_2 are present in a combustion environment in small amounts, their effect appears minimal. Limited studies indicate the SiO_2 scale is sufficient to protect against $SiCl_x(g)$ formation from HCl attack [86]. Attack of silicon-based ceramics is also negligible. Although SiS(g) formation is possible, this species is not very stable and the SiO_2 scale appears to protect against attack [87].

Low Level Metal Cation Impurities

In any type of combustion environment, low level metallic impurities are always present. These include sodium and potassium and also various transition metals such as iron. These are readily incorporated into the silica scale and generally open up the SiO_2 network leading to faster transport rates and enhanced oxidation rates [88, 89]. It appears that transport in SiO_2 is more readily affected by low level impurities than transport in the other common protective oxides, Al_2O_3 and Cr_2O_3.

Deposit-Induced Corrosion

As discussed in the Introduction, the burner rig studies have shown that salt-induced corrosion can lead to pitting and strength degradation. Salt deposits occur due to the interaction of sodium with sulfur fuel impurities [90]:

$$2\ NaCl(g) + SO_2(g) + 0.5\ O_2(g) + H_2O(g) = Na_2SO_4(l) + 2\ HCl(g) \qquad (10)$$

The dewpoint for Na_2SO_4 is a function of sulfur content, sodium content, and pressure. This is shown in Figure 26.23 [91]. Above the dewpoint, deposit-induced corrosion is minimal. However, below the dewpoint, deposition and the resulting corrosion can be quite serious.

Deposit induced corrosion only occurs under specific conditions. Figure 26.24 shows a coupon of SiC oxidized in burner rig with and without the addition of sodium [92]. Note the substantial amount of corrosion due to the sodium. These processes are best interpreted with the acid/base theory of oxides [91, 93]. Na_2SO_4 decomposes to Na_2O, which is the key reactant:

$$Na_2SO_4(l) = Na_2O(s) + SO_3(g) \quad (11)$$

The partial pressure of $SO_3(g)$ above the Na_2SO_4 deposit sets the chemical activity of Na_2O. A salt with a high activity of Na_2O is a basic molten salt; a salt with a low activity of Na_2O is an acidic molten salt. Since SiO_2 is an acidic oxide, it is readily attacked by a basic oxide to form sodium silicate:

$$2\ SiO_2(s) + Na_2O(s) = Na_2O{\cdot}2(SiO_2)(l) \quad (12)$$

This is the key reaction in deposit-induced corrosion of SiC and Si_3N_4. A basic oxide readily attacks the acidic SiO_2 and the protective film is replaced by a liquid, non-protective oxide film. Transport rates through the liquid film are rapid and more SiO_2 forms. This immediately reacts with the Na_2O to form more liquid and the thick film observed in Figure 26.24 forms. Clearly, this process can continue until all of the Na_2O is consumed.

The kinetics of this process are complex and depend on a variety of external (e.g. basic/acidic deposits) and internal factors [94]. In some cases, Na_2SO_4 is continuously deposited and hence a substantial quantity of SiC or Si_3N_4 can be consumed. In other cases, the amount of deposit may be limited and a sub-layer of silica grows below the melt. This would slow corrosion, but the consumption of SiC or Si_3N_4 can be quite substantial before this occurs.

In practice, the deposit is not only Na_2SO_4. Sea salt leads to a mixed Na_2SO_4, K_2SO_4, Ca_2SO_4, and $MgSO_4$ deposit [95]. This, in turn, may lead to other silicates besides sodium silicate [96]. Sodium vanadates may also deposit from lower purity fuels. The chemistry of these mixed deposits can be quite complex, but in general the basic solutions are very corrosive to silica. In addition it has been shown that carbon can drive an acidic sulfate deposit more basic [91]. This is significant, since carbon is a common additive in monolithic SiC and composites.

An important issue is the form of attack of the SiC and Si_3N_4. Attack does not occur with even recession, but rather in the form of localized pitting and attack at structural discontinuities [97]. This is illustrated in Figure 26.25. In general SiC tends to show more pitting and attack than Si_3N_4. Attack of Si_3N_4 is primarily along grain boundaries [98].

The type of surface attack described here is a problem with monolithic ceramics, since their strength is related to surface finish. In controlled laboratory studies significant strength degradation has been observed and fracture origins were often corrosion pits [17]. This is shown in Figures 26.26-27. This is consistent with the burner and engine testing programs, where similar observations have been made [10, 18].

Upper Temperature Limits

The question of upper temperature limits for the use of silicon-based ceramics is often raised. Typically these are 1300-1500°C in pure oxygen and are quite dependent on the material and system. The major environmental factors which impose a temperature limit are:

(1) Rapid oxidation rates, leading to extensive bubbling, and material consumption
(2) Rapid volatility and material consumption
(3) Scale/substrate reactions may lead to extensive bubbling in the scale. This is a particular issue for carbon-containing SiC [99].

Additive containing ceramics, which generally exhibit faster oxidation rates than pure materials in a high-velocity combustion environment would exhibit lower temperature limits than pure materials in pure oxygen. One approach to improve the oxidation behavior of additive-containing ceramics is a CVD coating of pure SiC or Si_3N_4.

As discussed, water vapor and salt deposits severely limit the upper use temperature for silicon-based ceramics. This attack is due to the nature of the SiO_2 film and hence a pure SiC or Si_3N_4 coating is not effective. For extended service at temperatures above about 1150°C in a turbine environment, which contains water vapor and the possibility of salt deposits, some type of environmental barrier coating (EBC) may be necessary. Several refractory oxides are being developed for this purpose. This is discussed in the next chapter of this book.

CORROSION MECHANISMS FOR OTHER CERAMICS

Aluminum Nitride

Aluminum nitride is often discussed as a potential high temperature material. It has a high thermal conductivity and forms an Al_2O_3 scale on oxidation. However, it failed catastrophically in some of the early engine tests [11]. It is known to rapidly oxidize in water vapor. Studies have shown that oxidation in water vapor leads to the formation of Al_2O_3 with micro-pores, which serve as rapid gas transport paths [100, 101]. This problem appears to be intrinsic to AlN and thus renders it unsuitable for combustion applications.

Oxides

Oxides are very often the most chemically stable compounds containing metallic elements [102]. As mentioned, the first ceramic materials considered for turbine engines were porcelains. The problem is that oxides may not be microstructurally stable to high temperatures and are also susceptible to thermal shock and creep. However, application of certain refractory oxide ceramic coatings on both metals and silicon-based ceramics may be a particularly promising approach for using ceramics in gas-turbine applications. Ceramic coatings are the topic of another chapter in this book.

As discussed, monolithic oxide ceramics are prime candidates for heat exchangers in automotive gas turbine (AGT) project [12]. Initially, lithium aluminum silicate (LAS) was proposed as a material for heat exchangers, however, LAS was quite susceptible to chemical attack. Lower temperature regions were attacked by small amounts of sulfuric acid in the combustion gas; higher temperature regions were attacked by the sodium or potassium impurities in the combustion gas. In both cases, ion exchange (H^+, Na^+, or K^+) occurred with the lithium, leading to an oxide with regions of different thermal expansion coefficient. This in turn led to cracking. As a result of these corrosion issues, magnesium aluminum silicate (MAS) was developed as a heat exchanger material. This material is substantially more chemically inert than LAS, but still appears to show some interactions with Na cations [103].

SUMMARY

From roughly 1970 to the present, there have been numerous programs to develop a ceramic heat engine. Although a commercially viable ceramic engine is not yet a reality, a good deal has been learned about the performance of ceramics in heat engine environments. Most of the emphasis has been on SiC and Si_3N_4 and, in recent years, on composites based on these materials. It has become apparent that the protective SiO_2 film which grows on these materials is not as inert as originally thought. While it is stable in an isothermal oxidizing environment, complications arise due to second phases in the ceramic substrate and exposure to complex combustion environments. These can be summarized as follows:

A. Material Issues
   1. Refractory oxide additives migrate to the SiO_2 scale and weaken its otherwise protective properties.
   2. Ceramic matrix composites contain an easily-oxidizable phase—either carbon fibers or carbon or boron nitride fiber coatings. Currently there is no adequate way to protect this

phase in the event of a matrix crack. Some types of sealing schemes have been developed, but more research is needed.

B. Environment Issues

1. Thermal cycling is not a major problem for the pure materials, but can lead to substantial degradation for the additive containing materials.
2. Water vapor can lead to substantial degradation both via enhanced oxidation and volatilization of the SiO_2 scale. In addition, boron-containing constituents are also quite susceptible to water vapor attack.
3. SiO_2 scales appear to be fairly impervious to HCl and SO_2.
4. Low level metallic impurities, such as Na and K, open the SiO_2 network and lead to faster oxidation rates. This is more of a problem for SiO_2 than other protective oxides.
5. Basic molten salt deposits readily dissolve the SiO_2 film, leading to a liquid, non-protective silicate. Attack of the SiC and Si_3N_4 is in the form of pitting and grain boundary attack, which leads to strength degradation.

Refractory oxide environmental barrier coatings may be a solution some of these issues and are discussed in more detail in the next chapter.

Other ceramics, such as AlN and MAS have also been considered for gas turbines. AlN is very reactive with water vapor and is therefore not suitable. MAS is a promising heat exchanger material, but reactivity with Na salts is a potential problem.

References:

[1] Jacobson, N. S., 1993, "Corrosion of Silicon-Based Ceramics in Combustion Environments," J. Am. Ceram. Soc., Vol. 76, pp. 3-28

[2] Conway, H. M., 1944, "The Possible Use of Ceramic Materials in Aircraft Propulsion Systems," NACA Report CB No. 4D10, NACA, Washington, D.C.

[3] Lay, L. A., 1991, "Corrosion Resistance of Technical Ceramics," 2nd Edition, Her Majesty's Stationary Office, London, pp. 18-23.

[4] Prochazka, S., 1974, "Sintering of Silicon Carbide," Ceramic High Performance Applications, Proceedings of the 2nd Army Material Technology Conference, Burke, J. J. et al, ed., Brook Hill Publ. Co, Chestnut Hill, MA, pp. 239-52.

[5] Riley, F. L., 2000, "Silicon Nitride and Related Materials," J. Am. Ceram. Soc., Vol. 83, pp. 245-65.

[6] Rice, R. W., 1981, "An Assessment of the Use of Ceramics in Heat Engines," Report 4499, Naval Research Laboratory, Washington, D.C.

[7] Singhal, S. C. and Lange, F. F., 1975, "Effect of Alumina Content on the Oxidation of Hot-Pressed Silicon Carbide," J. Am. Ceram. Soc., Vol. 58, pp. 433-35.

[8] Singhal, S. C., 1976, "Oxidation Kinetics of Hot-Pressed Silicon Carbide," J. Mat. Sci., Vol. 11, pp. 1246-53.

[9] Wallace, F. B., 1997, "Garrett-AiResearch Program Overview," Proceedings of the 1977 DARPA/NAVSEA Ceramic Gas Turbine Demonstration Engine Program Overview, Fairbanks, J. W. and Rice, R. W., eds., Metals and Ceramic Information Center, Columbus, OH, pp. 7-18.

[10] Richerson, D. W. and Yonushonis, T. M., 1978, "Environmental Effects on the Strength of Silicon-Nitride Materials," Proceedings of the 1977 DARPA/NAVSEA Ceramic Gas Turbine Demonstration Engine Program Overview, Fairbanks, J. W. and Rice, R. W., eds., Metals and Ceramic Information Center, Columbus, OH, pp. 247-71.

[11] Adams, J. W. and Larsen, D. C., 1984, "Evaluation of Corrosion/Erosion Behavior of Various Ceramic Materials," Report AFWAL-TR-84-4067, Air Force Wright Aeronautical Labs, Wright-Patterson Air Force Base, OH.

[12] Rahnke, C. J. and Vallance, J. K., 1977, "Reliability and Durability of Ceramic Regenerators in a Gas Turbine," Transactions of the ASME Journal of Engineering for Power, ASME Gas Turbine Conference, Philadelphia, PA, Paper No. 77-GT-59.

[13] Boyd, G. L., Kidwell, J. R., and Kreiner, D. M., 1987, "A Technology Development Summary for the AGT 101 Advanced Gas Turbine Program," Proceedings of the Twenty-Fourth Automotive Technology Development Contractors' Coordination Meeting, Society of Automotive Engineers, Inc., Warrendate, PA, P-197, pp. 115-35.

[14] Helms, H. E., Haley, P. J., Groseclose, L. E., Hilpisch, S. J., and Bell, A. H., 1989, "Advanced Turbine Technology Applications Project," Proceedings of the Twenty-Sixth Automotive Technology Development Contractors' Coordination Meeting, Society of Automotive Engineers, Inc., Warrendate, PA, P-219, pp. 319-26.

[15] Carruthers, W. D., Richerson, D. W., and Benn, K. W., 1980, "3500-Hour Durability Testing of Commercial Ceramic Materials Interim Report", DOE/NASA/0027-80/1, NASA Report CR-159785, NASA Lewis Research Center, Cleveland, OH.

[16] Lindberg, L. J., 1987, "Durability Testing of Ceramic Materials for Turbine Engine Applications," Proceedings of the Twenty-Fourth Automotive Technology Development Contractors' Coordination Meeting, Society of Automotive Engineers, Inc., Warrendate, PA, P-197, pp. 149-62.

[17] Smialek, J. L. and Jacobson, N. S., 1986, "Mechanism of Strength Degradation for Hot Corrosion of α-SiC," J. Am. Ceram. Soc., Vol. 60, pp. 741-52.

[18] Fox, D. S. and Smialek, J. L., 1990, "Burner Rig Hot Corrosion of Silicon Carbide and Silicon Nitride," J. Am. Ceram. Soc., Vol. 73, pp. 303-11.

[19] Federer, J. I., Ogle, J., Tennery, V. J., and Hensen, T., 1985, "Characterization of Corrosion Mechanisms Occurring in a Sintered SiC Exposed to Basic Coal Slags," J. Am. Ceram. Soc., Vol. 68, pp. 191-97.

[20] Seitz, E., 1994, "The German Materials Research Program 1985-1994," Advanced Performance Materials Vol. 1, pp. 87-117.

[21] Nickel, K. G., Danzer, R., Schneider, G., and Petzow, G., 1989, "Corrosion and Oxidation of Advanced Ceramics," Powder Metallurgy International, Vol. 21, pp. 29-34.

[22] Tatsumi, T., Takehara, I., and Ichikawa, Y., 1999, "Development Summary of the 300kW Ceramic Gas Turbine CGT302," ASME 96-GT-105.

[23] Yoshida, S., Tanaka, K., Terazono, H., Kubo, T., Hira, T., and Tsuruzono, S., 1999, "Development of Ceramic Components for CGT302," J. Gas Turbine Society of Japan, Vol. 27, pp. 322-28.

[24] Tanaka, K., Yoshida, M., Kubo, T., Terazono, H., and Tsuruzono, S., 2000, "Development and Evaluation of Ceramic Components for Small Gas Turbine Engines," International Gas Turbine and Aeroengine Congress and Exhibition, 2000-GT-531, American Society of Mechanical Engineers.

[25] Nakazawa, N., Sasaki, M., Nishiyama, T., Iwai, M., and Katagiri, H., 1997, "Status of the Automotive Ceramic Gas Turbine Development Program – Seven Years' Progress," International Gas Turbine and Aeroengine Congress and Exhibition, 97-GT-383, American Society of Mechanical Engineers.

[26] Yuri, I., Hisamatsu, T., Wanatabe, K., and Etori, Y., 1997, "Structural Design and High Pressure Test of a Ceramic Combustor for 1500°C Class Industrial Gas Turbine," Journal of Engineering for Gas Turbines and Power, Vol. 119, Transactions of the ASME, pp. 506-11.

[27] Machida, T., Nakayama, M., Wada, K., Hisamatsu, T., Yuri, I., and Watanabe, K., 1996, "Development of Ceramic Stator Vane for 1500°C Class Gas Turbine," International Gas Turbine and Aeroengine Congress and Exhibition, 96-GT-459, American Society of Mechanical Engineers.

[28] Hara, Y., Maeda, F., Tsuji, I., and Wada, K., 1991, "Development of Ceramic Components for a Power Generating Gas Turbine," ASME Gas Turbine Conference, Paper 91-GT-319.

[29] Kawamoto, H., 1995, "High Temperature Fracture Behavior of Structural Ceramics and Evaluation Technologies," JFCC Review No. 8, Japan Fine Ceramic Center, Nagoya, Japan, pp. 226-41.

[30] Misra, A. K., Johnson, A. M., Bartlett, B. J., 1999, "Progress Toward Meeting Material Challenges for High Speed Civil Transport Propulsion," Proceedings of the 14th International Symposium on Air Breathing Engines, Waltrup, P. J., ed., International Society for Air Breathing Engines, Chattanooga, TN.

[31] Office of Industrial Technologies, 1991, "Continuous Fiber Ceramic Composite Program," Report DOE/IET-91/8, Current Awareness Industrial Energy Technology, US Department of Energy, Washington, D.C.

[32] Robinson, R. C. and Smialek, J. L., 1999, "SiC Recession Caused by SiO_2 Scale Volatility under Combustion Conditions: I, Experimental Results and Empirical Model," J. Am. Ceram. Soc., Vol. 82, pp. 1817-25.

[33] Opila, E. J., Smialek, J. L., Robinson, R. C., Fox, D. S., and Jacobson, N. S., 1999, "SiC Recession Caused by SiO_2 Scale Volatility under Combustion Conditions: II, Thermodynamics and Gaseous Diffusion Model," J. Am. Ceram. Soc., Vol. 82, pp. 1826-34.

[34] Etori, Y., Hisamatsu, T., Yuri, I., Yasutomi, Y., Machida, T., and Wada, K., 1997, "Oxidation Behavior of Ceramics for Gas Turbines in Combustion Gas Flow at 1500°C," International Gas Turbine and Aeroengine Congress and Exhibition, 97-GT-355, American Society of Mechanical Engineers.

[35] Yuri, I., Hisamatsu, T., Etori, Y., and Yamamoto, T., 2000, "Degradation of Silicon Carbide in Combustion Gas Flow at High-Temperature and Speed," International Gas Turbine and Aeroengine Congress and Exhibition, 2000-GT-664, American Society of Mechanical Engineers.

[36] More, K. L., Tortorelli, P. F., Ferber, M. K., Walker, L. R., Keiser, J. R., Miriyala, N., Brentnall, W. D., and Price, J. R., 1999, "Exposure of Ceramics and Ceramic Matrix Composites in Simulated and Actual Combustor Environments," International Gas Turbine and Aeroengine Congress and Exhibition, 99-GT-292, American Society of Mechanical Engineers, New York.

[37] Miriyala, N., Simpson, J. F., Parathasarathy, and Brentnall, W. D., 1999, "The Evaluation of CFCC Liners after Field-Engine Testing in a Gas Turbine," International Gas Turbine and

Aeroengine Congress and Exhibition, 99-GT-395, American Society of Mechanical Engineers, New York.

[38] M. K. Ferber, H. T. Lin, V. Parthasarathy, and R.A. Wenglarz, "Degradation of Silicon Nitrides in High Pressure, Moisture Rich Environments," International Gas Turbine and Aeroengine Congress and Exhibition, 2000-GT-0661, American Society of Mechanical Engineers, New York.

[39] Lamouroux, F., Camus, G., and Thebault, J., 1994a, "Kinetics and Mechanisms of Oxidation of 2D Woven C/SiC Composites: I, Experimental Approach," J. Am. Ceram. Soc. Vol. 77, pp. 2049-57.

[40] Lamouroux, F., Naslain, R., and Jouin, J-M., 1994b, "Kinetics and Mechanisms of Oxidation of 2D Woven C/SiC Composites: II, Theoretical Approach," J. Am. Ceram. Soc. Vol. 77, pp. 2058-68.

[41] Filipuzzi, L., Camus, G., Naslain, R., and Thebault, J., 1994, "Oxidation Mechanisms and Kinetics of 1D-SiC/C/SiC Composite Materials: I, An Experimental Approach," J. Am. Ceram. Soc., Vol. 77, pp. 459-66.

[42] Filipuzzi, L., and Naslain, R., 1994, "Oxidation Mechanisms and Kinetics of 1D-SiC/C/SiC Composite Materials: II, Modeling," J. Am. Ceram. Soc., Vol. 77, pp.467-80.

[43] Ogbuji, L. U. J. T., 1998, "A Pervasive Mode of Oxidative Degradation in a SiC-SiC Composite," J. Am. Ceram. Soc., Vol. 81, pp. 2777-84.

[44] More, K. L., Tortorelli, P. F., Lin, H. T., Lara-Curzio, E., and Lowden, R. A., 1998, "Degradation Mechanisms of BN Interfaces in SiC/SiC Composites in Oxygen and Water-Vapor Containing Environments," Proceedings of the Symposium on High Temperature Corrosion and Materials Chemistry, Hou, P. Y., McNallan, M. J., Oltra, R., Opila, E. J., and Shores, D. A., Electrochemical Society, Pennington, NJ, pp. 382-94.

[45] Jacobson, N. S., Morscher, G. N., Bryant, D. R., and Tressler, R. E., 1999, "High-Temperature Oxidation of Boron Nitride: II, Boron Nitride Layers in Composites," J. Am. Ceram. Soc., Vol. 82, pp. 1473-82.

[46] Deadmore, D. L., Lowell, C. E., and Kohl, F. J., 1979, "The Effect of Fuel-to-Air Ratio on Burner Rig Hot Corrosion," Corrosion Science, Vol. 19, pp. 371-78.

[47] Ogbuji, L. U. J. T. and Opila, E. J., 1995, "A Comparison of the Oxidation Kinetics of SiC and Si_3N_4," J. Electrochem. Soc., Vol. 142, pp. 925-30.

[48] Opila, E. J. and Jacobson, N. S., 2000, "Corrosion of Ceramics," Corrosion and Environmental Degradation of Materials--Volume 19 of the Series: Materials Science and Technology, Schutze, M., ed., Wiley-VCH, Weinheim, Germany, pp. 327-88.

[49] Kofstad, P., 1988, "High Temperature Corrosion," Elsevier, London, pp. 17-18.

[50] Du, H., Tressler, R. E., and Spear, K. E., "Thermodynamics of the Si-N-O System and Kinetic Modeling of Oxidation of Si_3N_4," J. Electrochem. Soc., Vol. 136, pp. 3210-15.

[51] Ogbuji, L. U. J. T., Jayne, D. T., 1993, "Mechanism of Incipient Oxidation of Bulk Chemical Vapor Deposited Si_3N_4," J. Electrochem. Soc., Vol. 140, pp. 759-66.

[52] Fox, D. S., 1998, "Oxidation Behavior of Chemically-Vapor-Deposited Silicon Carbide and Silicon Nitride from 1200° to 1600°C," J. Am. Ceram. Soc., Vol. 81, pp. 945-50.

[53] Costello, J. A., and Tressler, R. E., 1986, "Oxidation Kinetics of Silicon Carbide Crystals and Ceramics: I, In Dry Oxygen," J. Am. Ceram. Soc., Vol. 69, pp 674-81.

[54] Cubiciotti, D., and Lau, K. H., 1978, "Kinetics of Oxidation of Hot-Pressed Silicon Nitride Containing Magnesia," J. Am. Ceram. Soc., Vol. 61, pp. 512-17.

[55] Cubiciotti, D., and Lau, K. H., 1979, "Kinetics of Oxidation of Yttria Hot-Pressed Silicon Nitride," J. Electrochem. Soc., Vol. 126, pp. 1723-28.

[56] Nickel, K. G., 1994, "Multiple Law Modeling for the Oxidation of Advanced Ceramics and a Model-Independent Figure-of-Merit," Corrosion of Advanced Ceramics, Nickel, K., ed., Kluwer Academic Publishers, Dordrecht, The Netherlands, pp. 59-72.

[57] Patel, J. K., Thompson, D. P., 1988, "The Low-Temperature Oxidation Problem in Yttria-Densified Silicon Nitride Ceramics," Br. Ceram. Trans. J., Vol. 87, pp. 70-73.

[58] Evans, A. G., Davidge, R. W., 1970, "The Strength and Oxidation of Reaction-Sintered Silicon Nitride," J. Mater. Sci., Vol. 5, p. 314.

[59] Porz, F., Thümmler, F., 1984, "Oxidation Mechanisms of Porous Silicon Nitride," J. Mater. Sci., Vol. 19, pp. 1283-95.

[60] Halbig, M. C. and Cawley, J. D., 2000, "Modeling the Environmental Effects on Carbon Fibers in a Ceramic Matrix at Oxidizing Conditions," Cer. Engr. Sci. Proc., Vol. 21, American Ceramic Society, Westerville, OH, pp. 219-26.

[61] Lamouroux, F., Bertrand, S., Pailler, R., and Naslain, R., 1999, "A Multilayer Ceramic Matrix for Oxidation Resistant Carbon-Fiber Reinforced CMCs," Key Engineering Materials, Vols 164-5, 365-8.

[62] Jacobson, N. S., Smialek, J. L., Fox, D. S., and Opila, E. J., 1995, "Durability of Silicon-Protected Ceramics in Combustion Environments," High-Temperature Ceramic Matrix Composites I: Design, Durability, and Performance, Ceramic Transactions, Volume 57, Evans, A. G. and Naslain, R., eds., American Ceramic Society, Westerville, OH, pp. 157-70.

[63] Eckel, A. J., Cawley, J. D., and Parthasarathy, T. A., 1995, "Oxidation Kinetics of a Continuous Carbon Phase in a Nonreactive Matrix," J. Am. Ceram. Soc., Vol. 78, pp. 972-80.

[64] Bhatt, R., 1989, "Oxidation Effects on the Mechanical Properties of SiC Fiber-Reinforced Reaction-Bonded Silicon Nitride Matrix Composites," NASA TM-102360, NASA Lewis Research Center, Cleveland, OH.

[65] Becher, P. F., 1983, "Strength Retention in SiC Ceramics after Long-Term Oxidation," J. Am. Ceram. Soc., Vol. 67, C-120-1.

[66] Jakus, K., Ritter, J. E., Jr., and Rogers, W. P., 1983, "Strength of Hot-Pressed Silicon Nitride After High Temperature Exposure," J. Am. Ceram. Soc., Vol. 67, pp. 471-75.

[67] Tressler, R. E., 1990, "Environmental Effects on the Long Term Reliability of SiC and Si_3N_4 Ceramics," Ceramic Transactions, Vol. 10, Corrosion and Corrosive Degradation of Ceramics, Tressler, R. E. and McNallan, M. J., eds., American Ceramic Society, Westerville, OH, pp. 99-124.

[68] Gogotsi, Y. G. and Grathwohl, G., 1993, "Stress-Enhanced Oxidation of Silicon Nitride Ceramics," J. Am. Ceram. Soc., Vol. 76, pp. 3093-104.

[69] Wereszczak, A. A., Ferber, M. K., Kirkland, T. P., More, K. L., Foley, M. R., and Yeckley, R. L., 1995, "Evaluation of Stress-Failure Resulting from High-Temperature Stress-Corrosion Cracking in a Hot Isostatically Pressed Silicon Nitride," J. Am. Ceram. Soc. Vol. 78, pp. 2129-40.

[70] Thümmler, F. and Grathwohl, F., 1989, "High Temperature Oxidation and Creep of Si_3N_4 and SiC Based Ceramics and their Mutual Interaction," in MRS International Meeting on Advanced Materials, Materials Research Society, pp. 237-53.

[71] Halbig, M. C., Brewer, D. N., Eckel, A. J., and Cawley, J. D., 1997. "Stressed Oxidation of C/SiC Composites," NASA TM 107457, National Aeronautics and Space Administration, Washington, DC.

[72] Lara-Curzio, E., Tortorelli, P. F., and More, K. L., 1997, "Stress-Rupture of Nicalon™/SiC at Intermediate Temperatures," Ceram. Engr. Sci. Proc., Vol. 18, American Ceramic Society, Westerville, OH, pp. 209-19.

[73] Morscher, G. N., Hurst, J., and Brewer, D., 2000, "Intermediate-Temperature Stress Rupture of a Woven Hi-Nicalon, BN-Interphase, SiC-Matrix Composite in Air," J. Am. Ceram. Soc., Vol. 83, pp. 1441-49.

[74] Gary, J. H., and Hardwick, G. E., 1975, Petroleum Refining: Technology and Economics, Marcel-Dekker, New York, p. 32.

[75] North American Combustion Handbook, 2nd Edition, 1978, North American Manufacturing Co., Cleveland, OH.

[76] Standard Specifications for Automotive Gasoline, ASTM Designation D, 1991, Book of ASTM Standards, American Society for Testing and Materials, Philadelphia, PA, pp. 439-89.

[77] Valkovic, V., 1978, Trace Elements in Petroleum, PPE Books, Tulsa, OK.

[78] Jungers, R. H., Lee, R. E., Jr., and van Lehmden, D. J., 1975, The EPA National Fuel Surveillance Network. I. Trace Constituents in Gasoline and Commercial Fuel Gasoline Additives, Environmental Health Perspectives, Vol. 10, pp. 143-50.

[79] Opila, E. J., 1994, "Oxidation Kinetics of Chemically Vapor-Deposited Silicon Carbide in Wet Oxygen," J. Am. Ceram. Soc., Vol. 77, pp. 730-36.

[80] Deal, B. E., and Grove, A. S., 1965, "General Relationship for the Thermal Oxidation of Silicon," J. Appl. Phys., Vol. 36, pp. 3770-78.

[81] Opila, E. J., 1999, "Variation of the Oxidation Rate of Silicon Carbide with Water-Vapor Pressure," J. Am. Ceram. Soc., Vol. 82, pp. 625-36.

[82] More, K. L., Tortorelli, P. F., Ferber, M. K., and Keiser, J. R., 2000 "Observations of Accelerated Oxidation of SiC at by Oxidation at High Water-Vapor Pressures, "J. Am. Ceram. Soc., Vol. 83, pp. 211-13.

[83] Hashimoto, A., 1992, "The effect of H_2O gas on volatilities of planet-forming major elements: I. Experimental determination of thermodynamic properties of Ca-, Al-, and Si-hydroxide gas molecules and its application to the solar nebula," Geochim. Cosmochim. Acta, Vol. 56, pp. 511-32.

[84] Opila, E. J., Fox, D. S., and Jacobson, N. S., 1997, "Mass Spectrometric Identification of Si-O-H(g) Species from the Reaction of Silica with Water Vapor at Atmospheric Pressure," J. Am. Ceram. Soc., Vol. 80, pp. 1009-12.

[85] Opila, E. J., and Nguyen, Q. N., 1998, "Oxidation of Chemically-Vapor-Deposited Silicon Carbide in Carbon Dioxide," J. Am. Ceram. Soc., Vol. 81, pp. 1949-52.

[86] Marra, J. E., Kreidler, E. R., Jacobson, N. S. and Fox, D. S., 1988, "Reactions of Silicon-Based Ceramics in Mixed Oxidation Chlorination Environments," J. Am. Ceram. Soc., Vol. 71, pp. 1067-73.

[87] Nickel, H. and Förthmann, R., 1994, "Hot Gas Corrosion of Structural Ceramics," Corrosion of Advanced Ceramics, Nickel, K., ed., Kluwer Academic Publishers, Dordrecht, The Netherlands, pp. 99-116.

[88] Pareek, V., Shores, D. A., 1991, "Oxidation of Silicon Carbide in Environments Containing Potassium Salt Vapor," J. Am. Ceram. Soc., Vol. 74, pp. 556-63.

[89] Zheng, Z., Tressler, R. E., and Spear, K. E., 1992, "The Effect of Sodium Contamination on the Oxidation of Single Crystal Silicon Carbide, Corrosion Science, Vol. 33, pp. 545-56.

[90] Kohl, F. J., Stearns, C. A., and Fryburg, G. C., 1975, "Sodium Sulfate: Vaporization Thermodynamics and Role in Corrosive Flames," Proceedings, Metal-Slag-Gas Reactions and Processes, Foroulis, Z. A. and Smeltzer, W. W., eds., The Electrochemical Society, Princeton, NJ, pp. 649-64.

[91] Jacobson, N. S., 1989, "Sodium Sulfate: Deposition and Dissolution of Silica," Oxid. Met., Vol. 31, pp. 91-103.

[92] Jacobson, N. S., Stearns, C. A., and Smialek, J. L., 1988, "Burner Rig Corrosion of SiC at 1000°C," Adv. Ceram. Mat., Vol. 1, pp. 154-61.

[93] Rapp, R. A., 1986, "Chemistry and Electrochemistry of the Hot Corrosion of Metals," Corros. Sci., Vol. 42, pp. 568-77.

[94] Berthold, C. and Nickel, K. G., 1998, "Hot-Corrosion Behaviour of Silica and Silica-Formers: External vs. Internal Control," Journal of the European Ceramic Society, Vol. 5, pp. 2365-72.

[95] Bornstein, N. M., 1996, "Reviewing Sulfidation Corrosion—Yesterday and Today," JOM, Vol. 11, pp. 37-39.

[96] Fox, D. S., Cuy, M. D., and Nguyen, Q. N., 1998, "Sea-Salt Corrosion and Strength of a Sintered α-Silicon Carbide," J. Am. Ceram. Soc., Vol. 81, pp. 1565-70.

[97] Jacobson, N. S. and Smialek, J. L., 1986, "Corrosion Pitting of SiC by Molten Salts," J. Electrochem. Soc., Vol. 133, pp. 2615-21.

[98] Jacobson, N. S., Smialek, J. L., and Fox, D. S., 1990, "Molten Salt Corrosion of SiC and Si_3N_4," Handbook of Ceramics and Composites Volume I: Synthesis and Properties, Cheremisinoff, N. P., ed., Marcel Dekker, New York, pp. 99-137.

[99] Jacobson, N. S., Lee, K. N., and Fox, D. S., 1992, "Reactions of Silicon Carbide and Silicon Oxide at Elevated Temperatures," J. Am. Ceram. Soc., Vol. 75, pp. 1603-11.

[100] Sato, T., Haryu, K., Endo, T., and Shimada, M., 1987, "High temperature oxidation of hot-pressed aluminum nitride by water vapor," J. Mater. Sci., Vol. 22, pp. 2277-80.

[101] Opila, E., Jacobson, N., Humphrey, D., Yoshio, T., and Oda, K., 1998, "The Oxidation of AlN in Dry and Wet Oxygen," Proceedings of the Symposium on High Temperature Corrosion and Materials Chemistry, Vol. 98-9, Hou, P. Y., et al., eds., The Electrochemical Society, Pennington, NJ, pp. 430-37.

[102] Searcy, A. W., 1970, "Enthalpy and Predictions of Solid-State Reaction Equilibria," Chemical and Mechanical Behavior of Inorganic Materials, Searcy, A. W., Ragone, D. V., and Colombo, U., eds., Wiley-Interscience, New York, pp. 33-55.

[103] Bianco, R. and Jacobson, N., 1989, "Corrosion of Cordierite Ceramics by Sodium Sulfate at 1000°C," J. Mater. Sci., Vol. 24, pp. 2903-10.

Table 26-I.

Properties of Some Common Hydrocarbon Fuels.

Fuel	Boiling Range (K) [74]	H:C Molar Ratio [75]	S Content (w/o) [76, 77]	Na + K content (ppm) [77]	V content (ppm) [78]
Unleaded Automotive Gasoline	300-375	2.02	0.15	3.6	<0.003
Jet A (Commercial Aviation Fuel)	450-560	1.92	0.05	~10	0.06
Fuel Oils	450-615	1.61	0.1-1.0	10-20	<300

Figure Captions

26.1. Common degradation modes for high temperature turbine components in an aircraft turbine engine (adapted from Jacobson [1]).

26.2. Schematic of NASA Glenn Research Center burner rig used for studying oxidation and corrosion of high temperature materials in actual combustion environments (Jacobson [1], reprinted with permission of the American Ceramic Society).

26.3. Baseline oxidation rates for pure SiC and Si_3N_4 in pure oxygen (adapted from Ogbuji and Opila [47], reprinted with permission of Wiley-VCH).

26.4. Oxidation behavior at 1370°C for SiC hot pressed with varying amounts of Al_2O_3 in 1 atm of dry oxygen (Singhal and Lange [7], reprinted with permission from the American Ceramic Society).

26.5. Y_2O_3 containing Si_3N_4 oxidized for 97 h at 1300°C in dry oxygen (Jacobson [1], reprinted with permission from the American Ceramic Society). The bright particles are the yttrium-silicate phase within the silica.

26.6. Schematic of fiber reinforced ceramic matrix composite (Jacobson, et al. [62], reprinted with permission from the American Ceramic Society).

26.7. Weight change curves for oxidation of SiC fiber/Si_3N_4 matrix composites (adapted from Bhatt [64]).

26.8. Schematic for oxidation model of a carbon coated SiC fiber in a SiC matrix (adapted from Filipuzzi and Naslain [42], reprinted with permission from Wiley-VCH).

26.9. Two oxidation processes of a BN coated SiC fiber in a SiC matrix (a) Borosilicate glass formation after oxidation at 816°C in oxygen for 100 h (b)Volatilization of BN due to water vapor interactions after oxidation at 500°C in humid air (Jacobson, et al. [45], reprinted with permission from the American Ceramic Society).

26.10. Schematic for water vapor volatilization of a BN fiber coating in a SiC fiber/SiC matrix (Jacobson, et al. [45], reprinted with permission from the American Ceramic Society).

26.11. Combustion products and adiabatic flame temperature for the combustion of Jet A fuel in air (Jacobson [1], reprinted with permission from the American Ceramic Society).

26.12. Thermal expansion of SiC, Si_3N_4, amorphous SiO_2, and crystalline SiO_2 as a function of temperature (Opila and Jacobson [48], reprinted with permission from Wiley-VCH).

26.13. Cyclic oxidation weight change kinetics for several silica forming materials in air at 1300°C in 5 h cycles (Opila and Jacobson [48], reprinted with permission from Wiley-VCH).

26.14. Model paralinear kinetics for SiC oxidized in water vapor. Calculated results are typical of exposures at 1200°C in 50% H_2O/50% O_2 at flow rates of 4.4 cm/s (Opila and Jacobson [48], reprinted with permission from Wiley-VCH).

26.15. Oxidation/volatilization weight change kinetics for silica, CVD SiC and CVD Si_3N_4 at 1200°C in 50% H_2O/50% O_2 at flow rates of 4.4 cm/s (Opila and Jacobson [48], reprinted with permission from Wiley-VCH).

26.16. Weight loss of CVD SiC in a fuel-lean high pressure burner rig with gas velocities of 20 m/s. (Adapted from Robinson and Smialek [32], reprinted with permission from Wiley-VCH).

26.17. Normalized weight loss results of CVD SiC in a fuel-lean high pressure burner rig with gas velocities of 10-27 m/s and total pressures between 5 and 15 atm. (Adapted from Robinson and Smialek [32], reprinted with permission from Wiley-VCH).

26.18 SiC/SiC combustor liner utilized in an industrial gas turbine operated for about 2300h at a total pressure of 10 atm and a peak liner temperature of 1150°C. The micrographs show an intact SiC seal coat from the cooler portions of the liner. The SiC seal coat is breached resulting in a glassy reaction zone in the hot section of the liner. The micron bar is equal to 100μm. (courtesy of M.K. Ferber, Oak Ridge National Laboratory).

26.19 Measurement of recession of AS800 Si_3N_4 vanes at the mid-span of the trailing edge tested in an industrial gas turbine operated for 815h at a total pressure of 8.9 atm and a peak temperature of 1260°C (open circles). The lines represent predictions based on the model developed in [32] (Ferber et al. [38]).

26.20 Profile of the cross-section at mid-span of an AS800 Si_3N_4 vane before and after engine testing in an industrial gas turbine operated for 815h at a total pressure of 8.9 atm and a peak temperature of 1260°C (Ferber et al. [38]).

26.21 Profile of the leading edge of an AS800 Si_3N_4 vane at mid-span before and after engine testing in an industrial gas turbine operated for 815h at a total pressure of 8.9 atm and a peak temperature of 1260°C. Vane is ~2.5 cm long. (courtesy of M.K. Ferber, Oak Ridge National Laboratory).

26.22. Comparison of CVD SiC oxidation kinetics in the oxidants CO_2, O_2 and H_2O at 1200°C. (Opila and Nguyen [85], reprinted with permission from the American Ceramic Society).

26.23. Dew points for the deposition of Na_2SO_4 (Jacobson [1], reprinted with permission from the American Ceramic Society).

26.24. Optical micrographs of sintered SiC coupons with carbon and boron additives, oxidized in a 4 atm pressurized burner rig at 1000°C (a) 46 h with no sodium (b) 13.5 h with a NaCl-seeded flame (Jacobson [1] reprinted with permission from the American Ceramic Society).

26.25. Sequence showing sintered SiC (a) before corrosion (b) after corrosion with $Na_2SO_4/(10^{-4}$ bar SO_3 + 1 bar $O_2)$, 1273 K for 48 h (c) with corrosion products removed, revealing pitting (Jacobson [1], reprinted with permission from the American Ceramic Society).

26.26. Strength degradation of SiC after burner rig corrosion (adapted from Jacobson, et al. [98]). SASC (B,C) = Sintered α-SiC with boron and carbon additives; RBSC = Reaction Bonded SiC.

26.27. Typical fracture origin from burner rig corrosion in SiC (adapted from Jacobson, et al. [98]). The enlargements show the glass-filed pit and the pit after an hydrofluoric acid treatment to remove the glass.

Schematic Diagram of Turbofan Engine

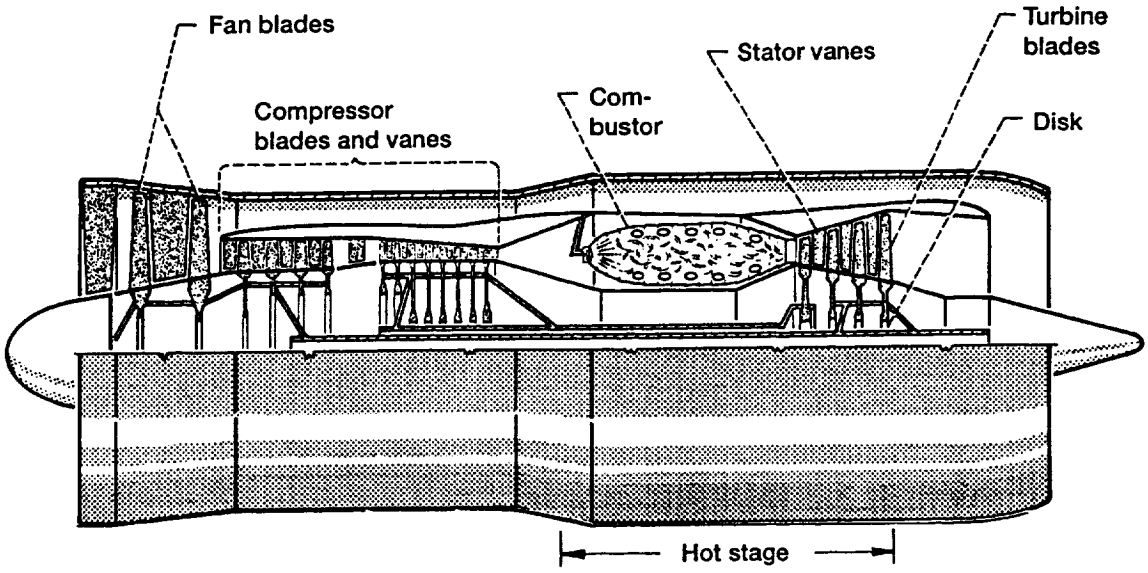

Component	Typical Operating Conditions			Critical Problems
	Temperature (°C)	Stress (MPa)	Life (hr)	
Blades	900 - 1050	140 - 210	5000	Creep strength, stability, oxidation, hot corrosion, thermal fatigue
Vanes	950 - 1100	35 - 70	5000	Thermal fatigue, oxidation, hot corrosion
Disks	400 - 650	420 - 1050	15 000	Low cycle fatigue
Combustors	850 - 1100	20 - 35	4000	Thermal fatigue, oxidation

E-12413 Jacobson 9pt/100% nm from CD-00-79951

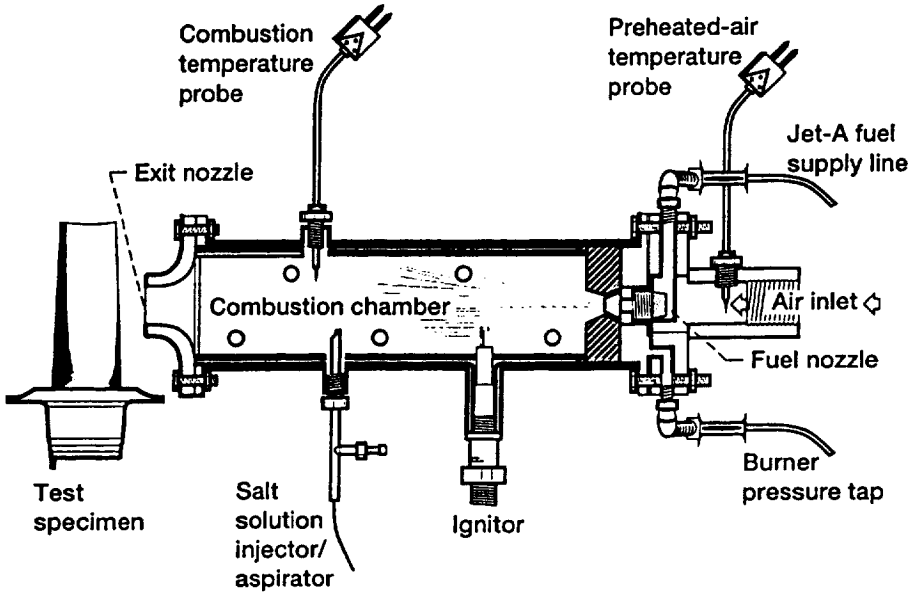
Combustion temperature probe
Preheated-air temperature probe
Jet-A fuel supply line
Exit nozzle
Combustion chamber
Air inlet
Fuel nozzle
Burner pressure tap
Test specimen
Salt solution injector/ aspirator
Ignitor

Figure 26.2

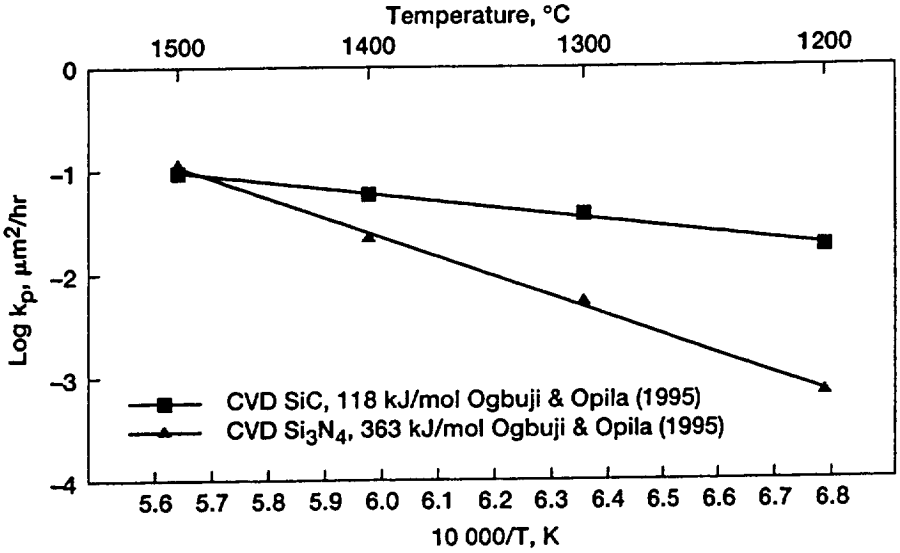
Temperature, °C
1500
1400
1300
1200
0
−1
−2
−3
−4
Log k_p, μm²/hr
CVD SiC, 118 kJ/mol Ogbuji & Opila (1995)
CVD Si_3N_4, 363 kJ/mol Ogbuji & Opila (1995)
5.6 5.7 5.8 5.9 6.0 6.1 6.2 6.3 6.4 6.5 6.6 6.7 6.8
10 000/T, K

Figure 26.3

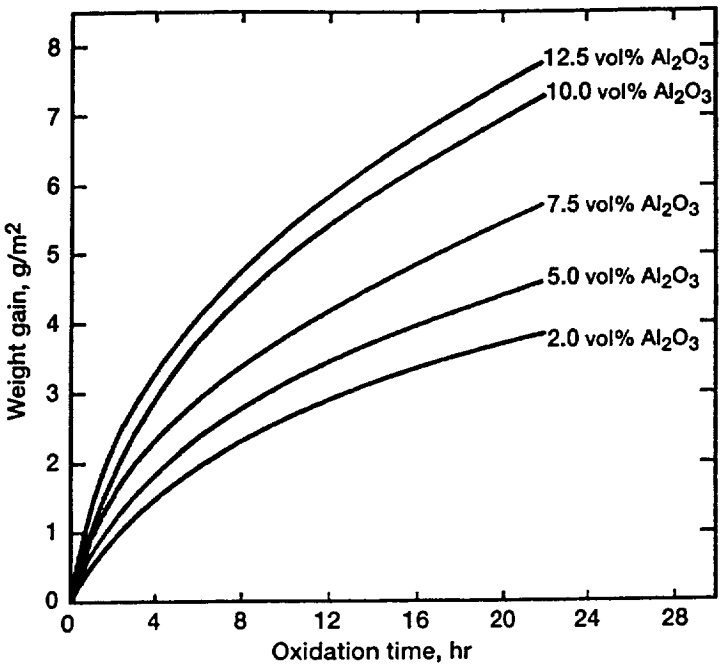
12.5 vol% Al_2O_3
10.0 vol% Al_2O_3
7.5 vol% Al_2O_3
5.0 vol% Al_2O_3
2.0 vol% Al_2O_3
Weight gain, g/m^2
Oxidation time, hr
0
1
2
3
4
5
6
7
8
0
4
8
12
16
20
24
28

Figure 26.4

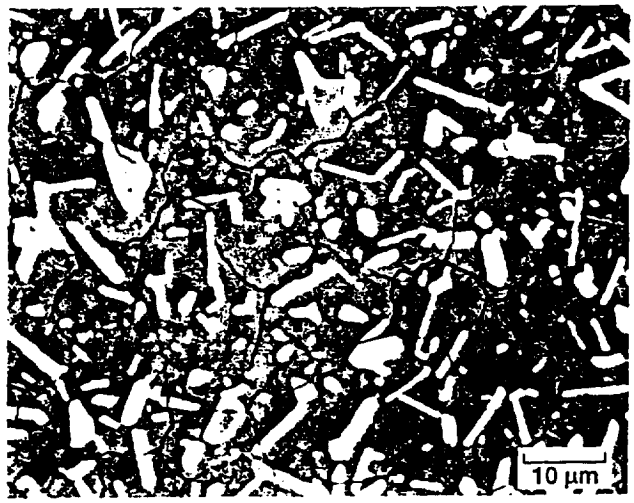

Figure 26.5

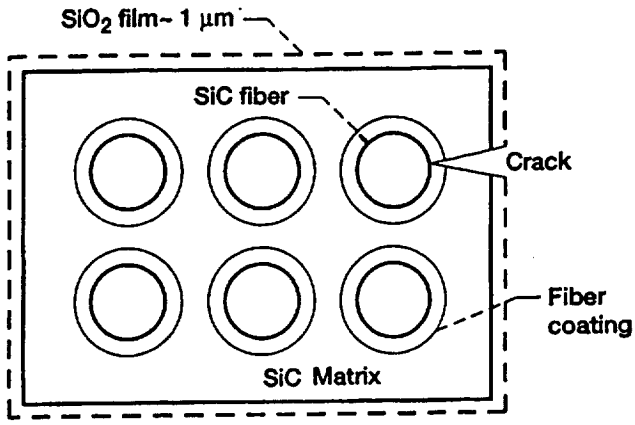

Figure 26.6

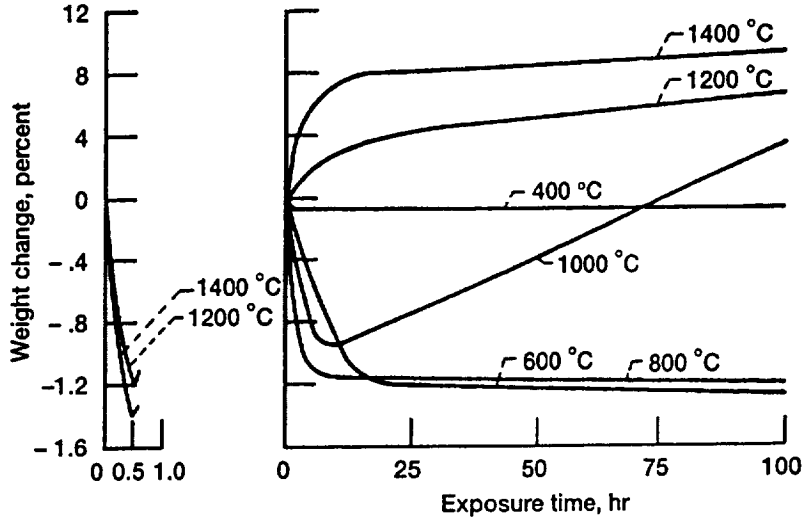

Figure 26.7

E-12413 Jacobson 9pt/100% nm from E-11463 fig 52 scan

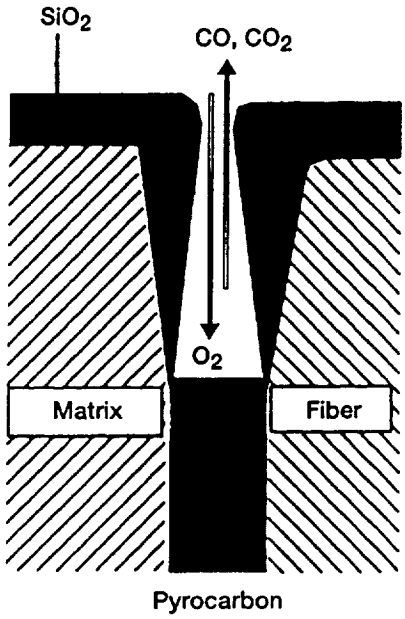

Figure 26.8

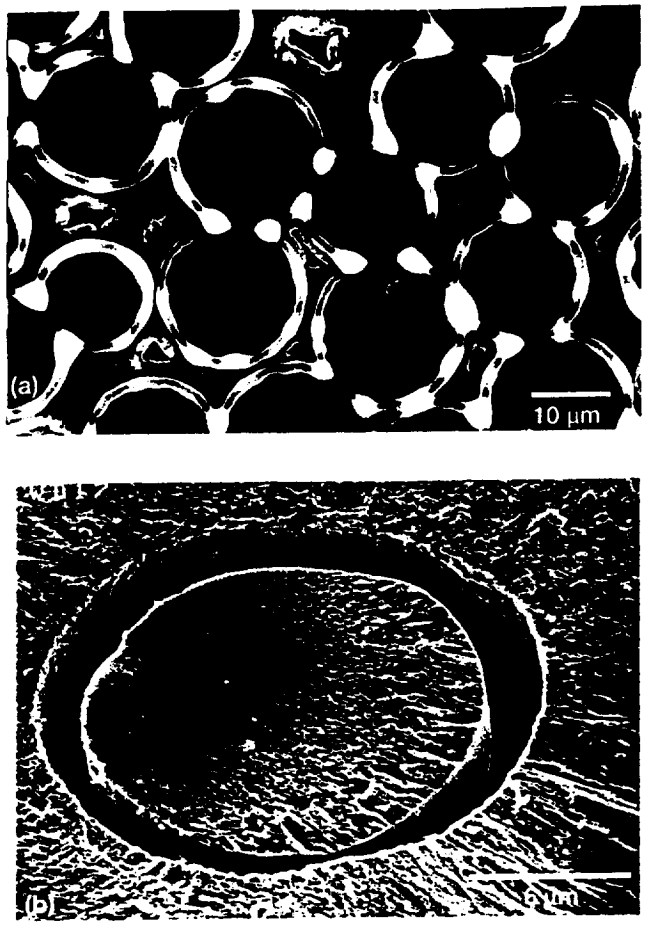

Figure 26.9

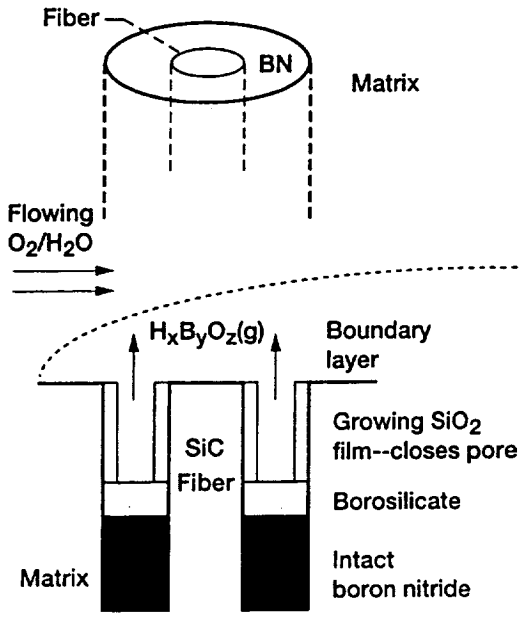
Fiber
BN
Matrix
Flowing
O_2/H_2O
$H_xB_yO_z(g)$
Boundary
layer
Growing SiO_2
film--closes pore
SiC
Fiber
Borosilicate
Intact
boron nitride
Matrix

Figure 26.10

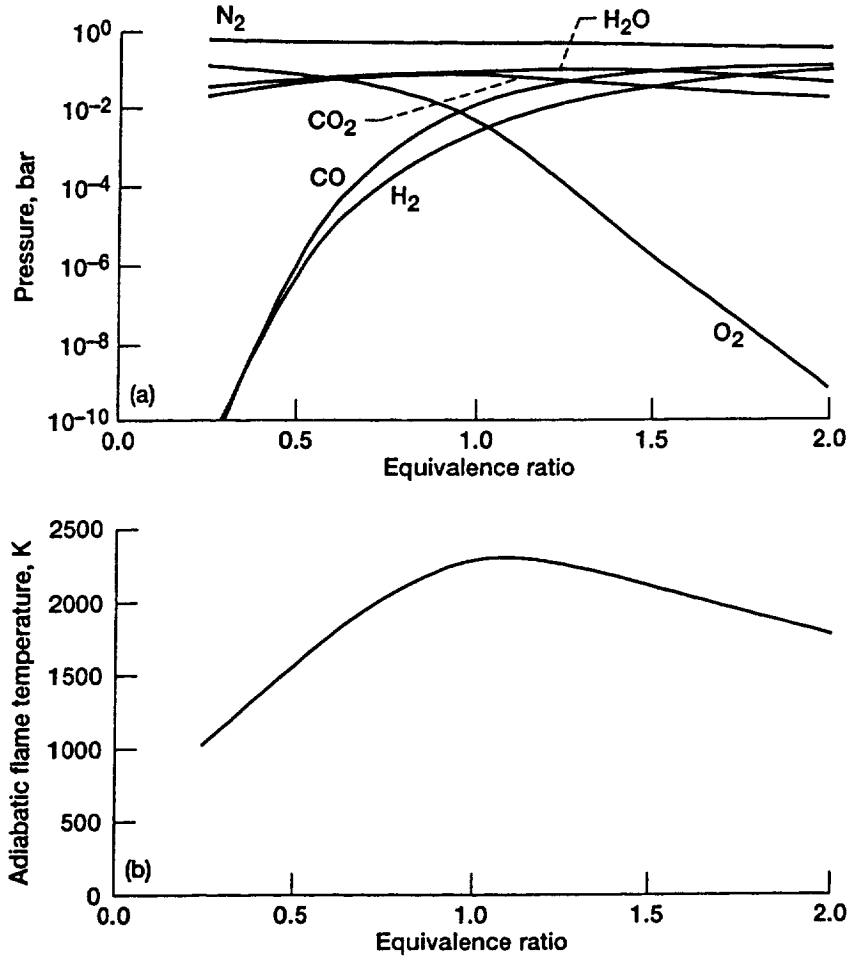
N_2
H_2O
CO_2
CO
H_2
O_2
Pressure, bar
10^0
10^{-2}
10^{-4}
10^{-6}
10^{-8}
10^{-10}
(a)
0.0
0.5
1.0
1.5
2.0
Equivalence ratio
Adiabatic flame temperature, K
2500
2000
1500
1000
500
0
(b)
0.0
0.5
1.0
1.5
2.0
Equivalence ratio

Figure 26.11

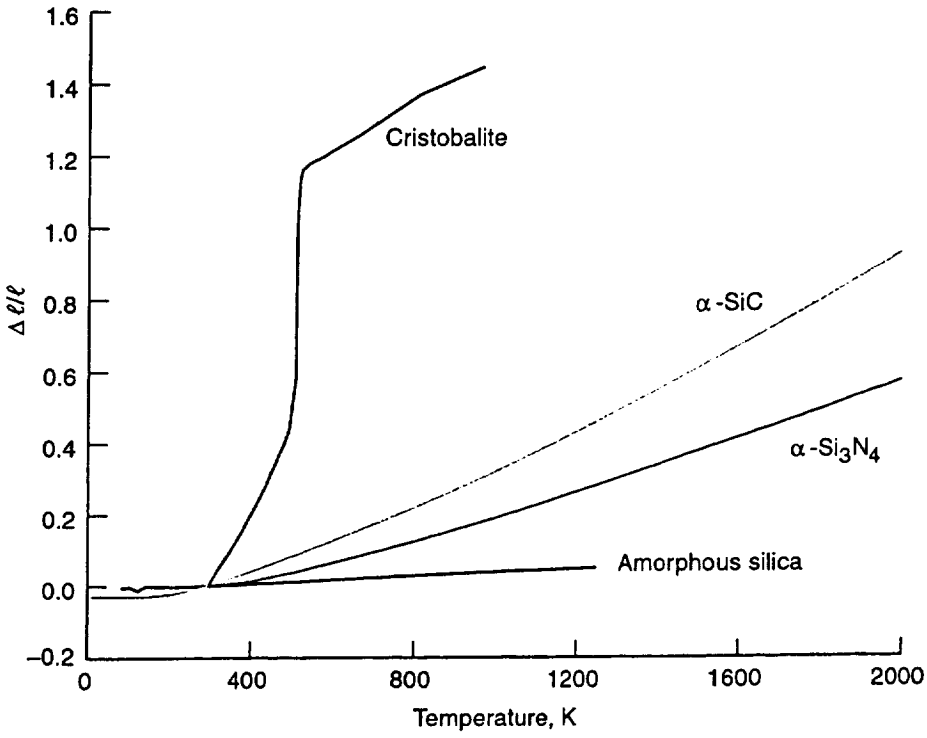
1.6
1.4
1.2
1.0
0.8
0.6
0.4
0.2
0.0
−0.2
Δℓ/ℓ
Cristobalite
α-SiC
α-Si3N4
Amorphous silica
0
400
800
1200
1600
2000
Temperature, K

Figure 26.12

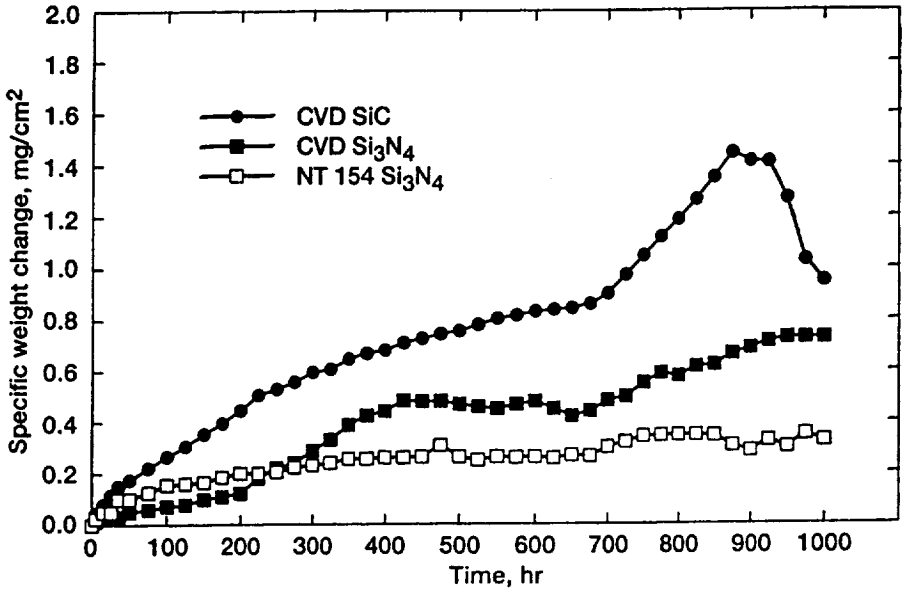
Specific weight change, mg/cm^2
2.0
1.8
1.6
1.4
1.2
1.0
0.8
0.6
0.4
0.2
0.0
0
100
200
300
400
500
600
700
800
900
1000
Time, hr
CVD SiC
CVD Si_3N_4
NT 154 Si_3N_4

Figure 26.13

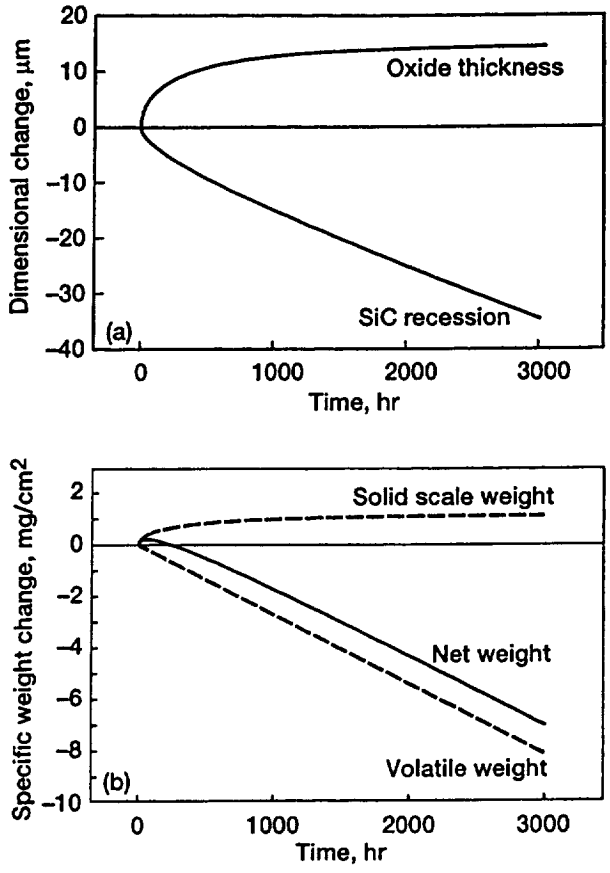
Dimensional change, μm
20
10
0
−10
−20
−30
−40
Oxide thickness
SiC recession
(a)
0
1000
2000
3000
Time, hr
Specific weight change, mg/cm²
2
0
−2
−4
−6
−8
−10
Solid scale weight
Net weight
Volatile weight
(b)
0
1000
2000
3000
Time, hr

Figure 26.14

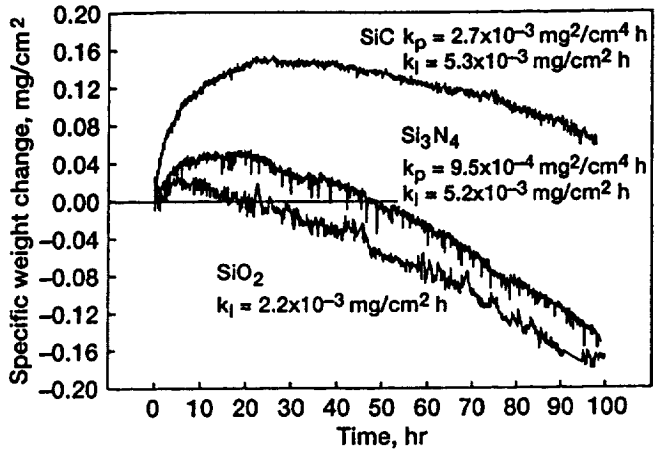
Specific weight change, mg/cm²
0.20
0.16
0.12
0.08
0.04
0.00
−0.04
−0.08
−0.12
−0.16
−0.20
0 10 20 30 40 50 60 70 80 90 100
Time, hr
SiC $k_p = 2.7x10^{-3}$ mg²/cm⁴ h
$k_l = 5.3x10^{-3}$ mg/cm² h
Si_3N_4
$k_p = 9.5x10^{-4}$ mg²/cm⁴ h
$k_l = 5.2x10^{-3}$ mg/cm² h
SiO_2
$k_l = 2.2x10^{-3}$ mg/cm² h

Figure 26.15

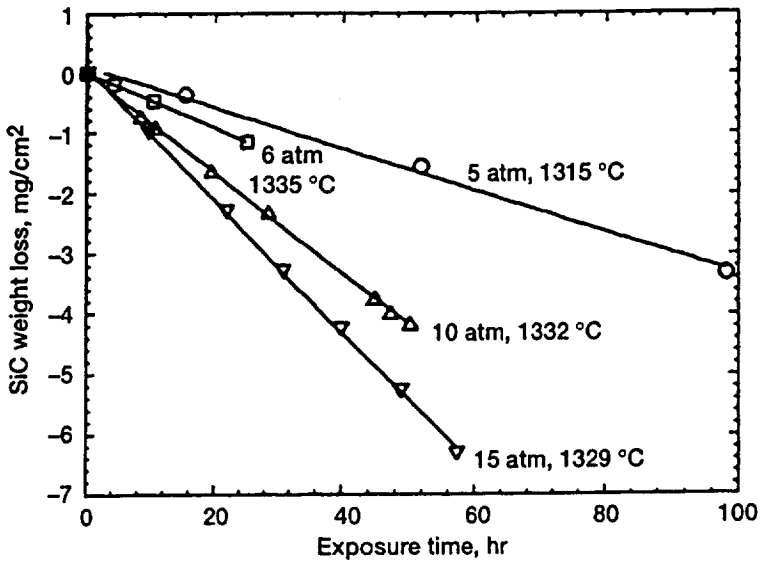
SiC weight loss, mg/cm2
1
0
-1
-2
-3
-4
-5
-6
-7
0
20
40
60
80
100
Exposure time, hr
6 atm
1335 °C
5 atm, 1315 °C
10 atm, 1332 °C
15 atm, 1329 °C

Figure 26.16

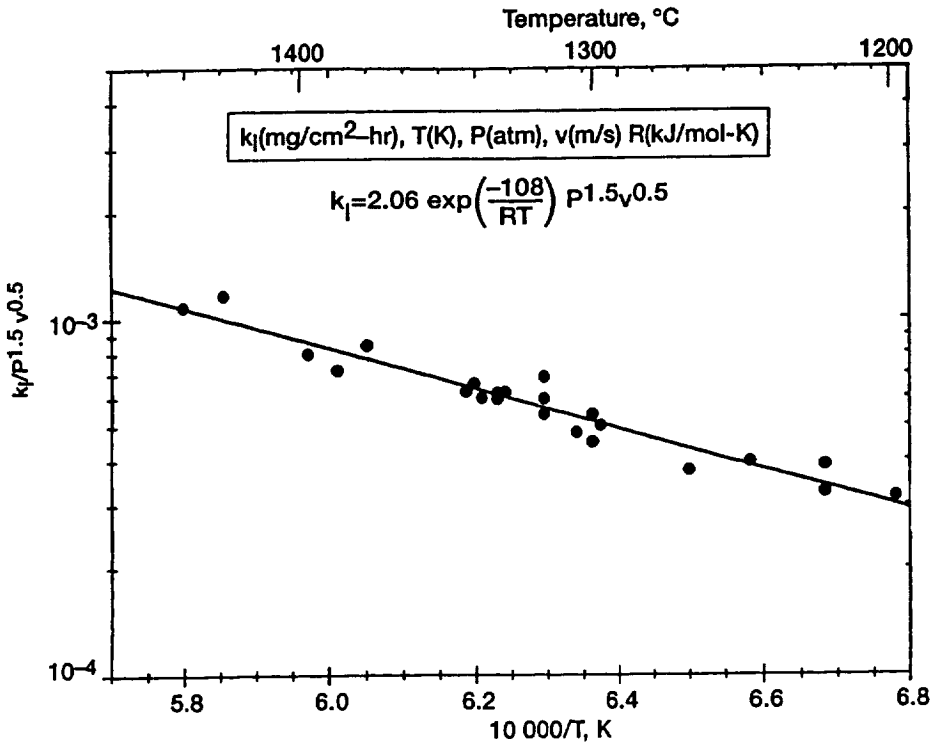
Temperature, °C
1400
1300
1200
k_l(mg/cm^2–hr), T(K), P(atm), v(m/s) R(kJ/mol-K)
$k_l = 2.06 \exp\left(\frac{-108}{RT}\right) P^{1.5} v^{0.5}$
$k_l/P^{1.5}v^{0.5}$
10^{-3}
10^{-4}
5.8
6.0
6.2
6.4
6.6
6.8
10 000/T, K

Figure 26.17

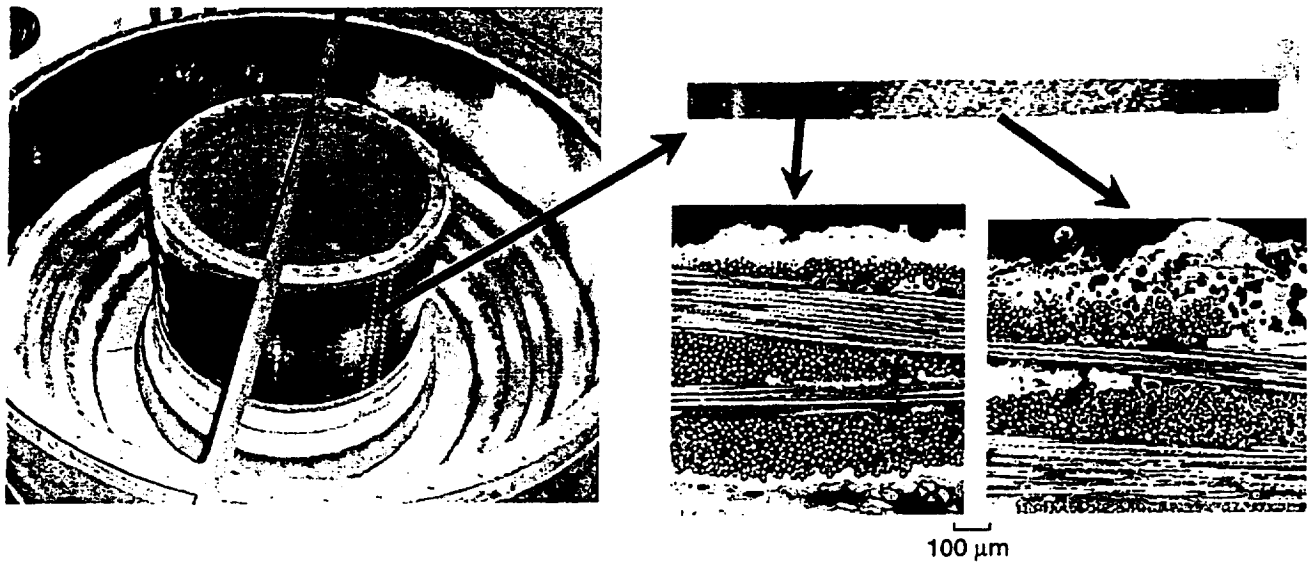

Figure 26.18

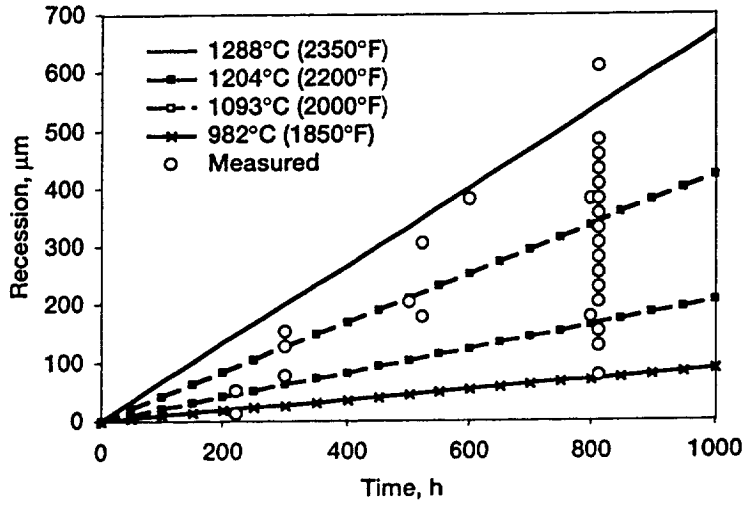
1288°C (2350°F)
1204°C (2200°F)
1093°C (2000°F)
982°C (1850°F)
Measured
Recession, µm
Time, h
0
100
200
300
400
500
600
700
0
200
400
600
800
1000

Figure 26.19

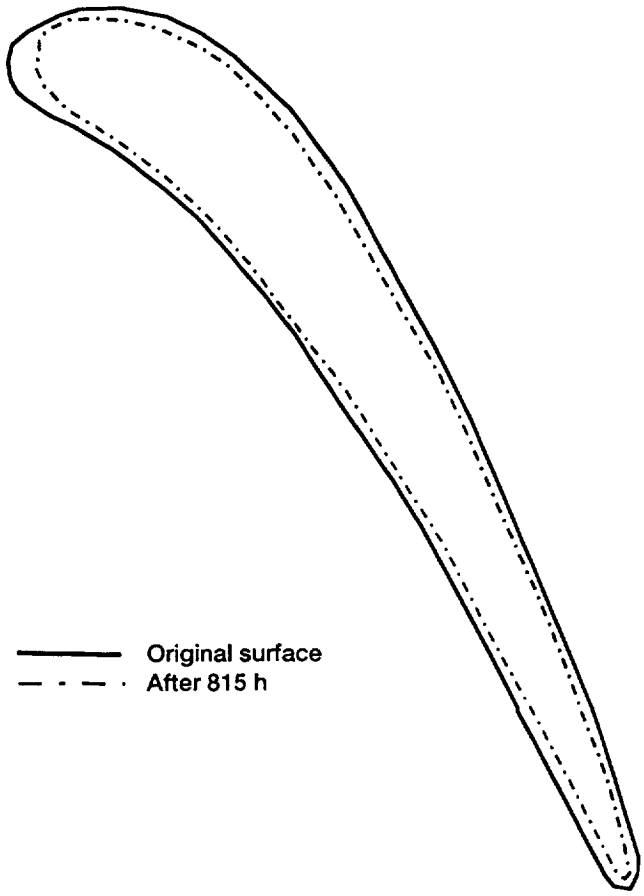

Figure 26.20

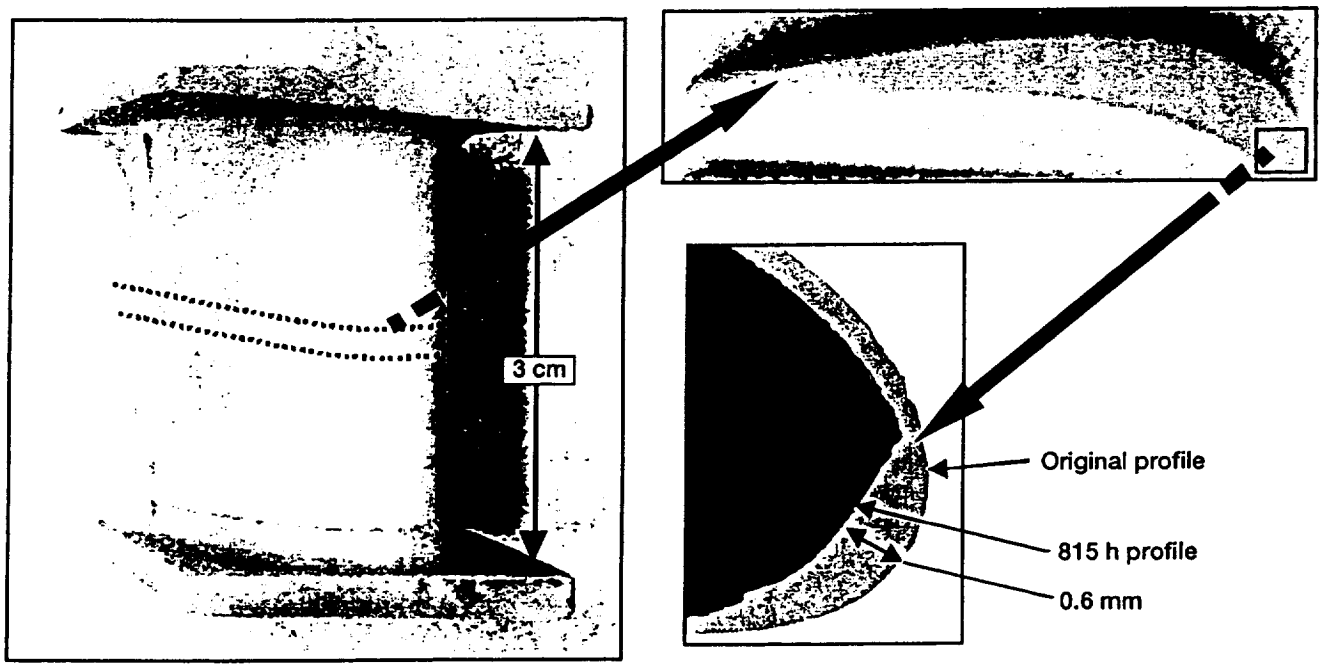

Figure 26.21

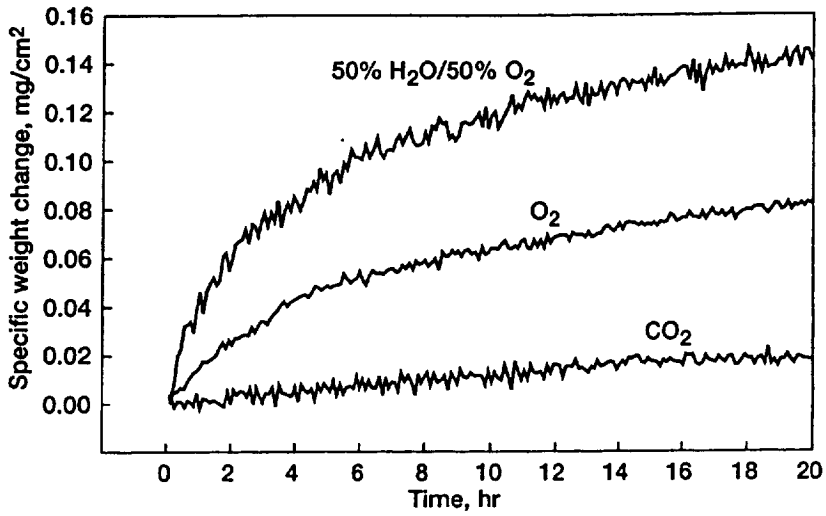
Specific weight change, mg/cm²
0.16
0.14
0.12
0.10
0.08
0.06
0.04
0.02
0.00
50% H2O/50% O2
O2
CO2
0
2
4
6
8
10
12
14
16
18
20
Time, hr

Figure 26.22

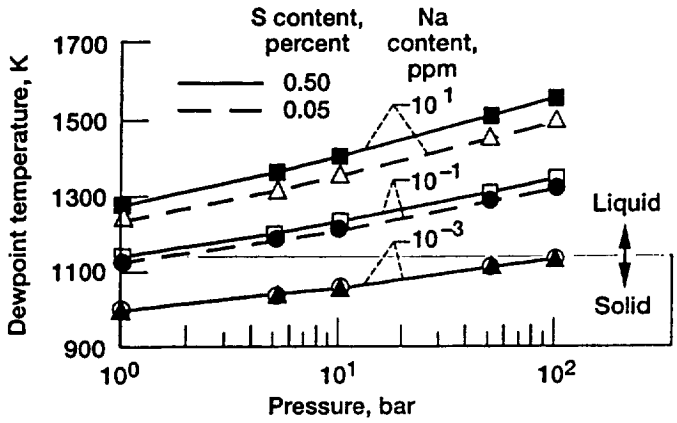
S content, percent
0.50
0.05
Na content, ppm
10^1
10^{-1}
10^{-3}
Liquid
Solid
Dewpoint temperature, K
1700
1500
1300
1100
900
10^0
10^1
10^2
Pressure, bar

Figure 26.23

Figure 26.24

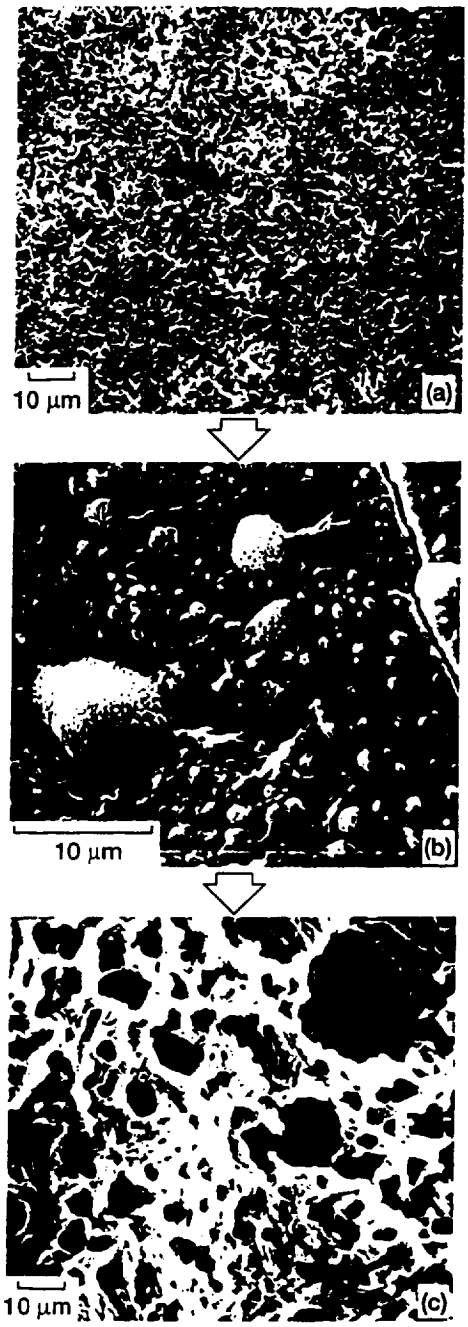

Figure 26.25

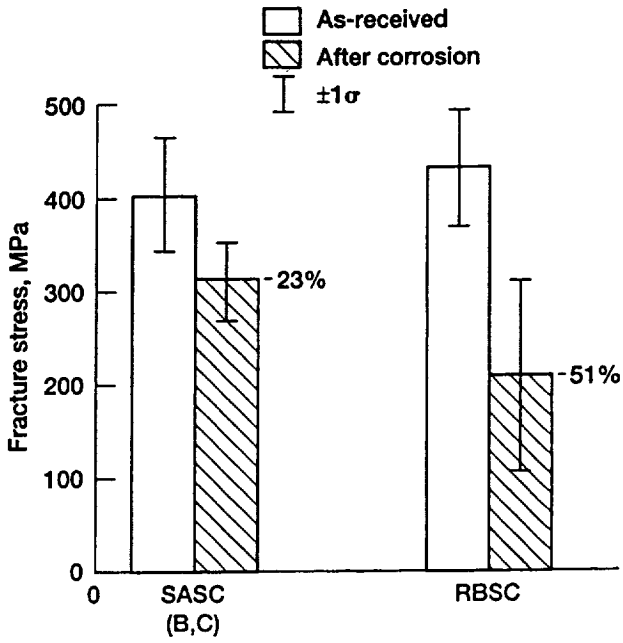
As-received
After corrosion
±1σ
Fracture stress, MPa
500
400
300
200
100
0
0
SASC
(B,C)
RBSC
23%
51%

Figure 26.26

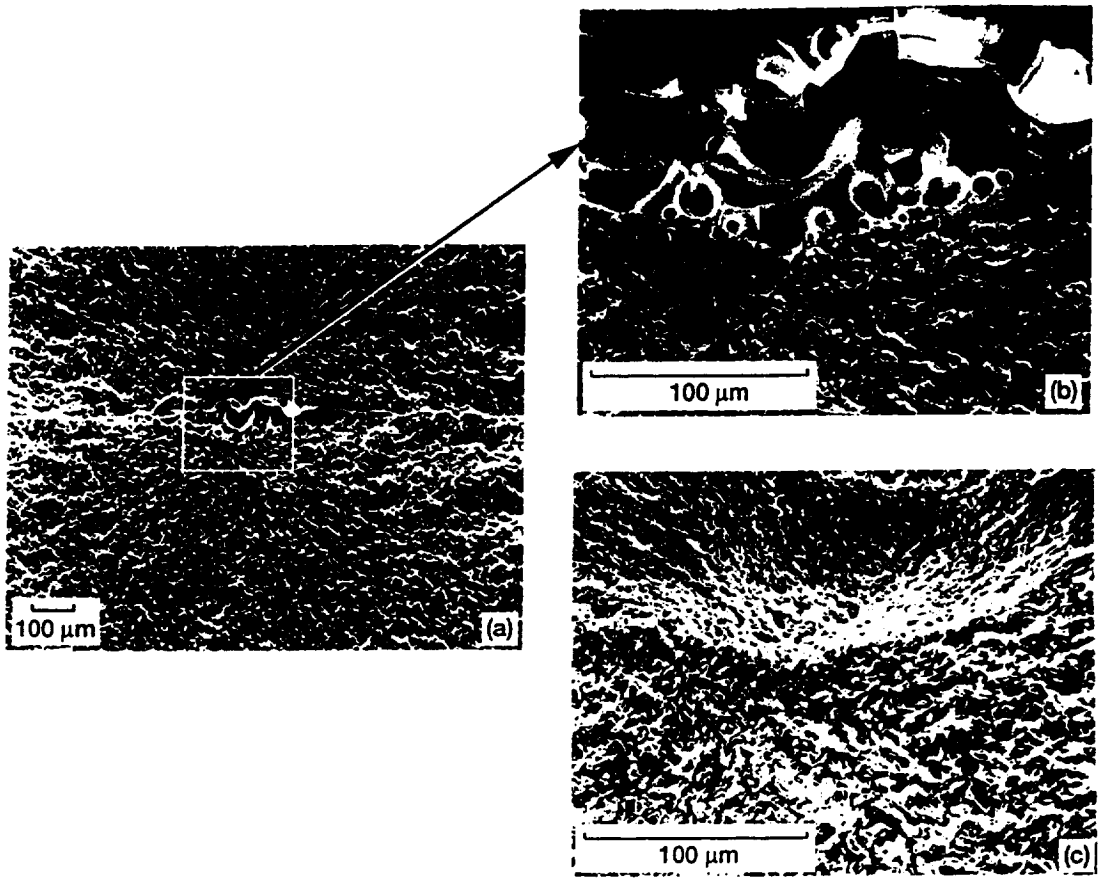

Figure 26.27